Chapter 3 Geochemical Prospecting

3-1 Re-examination of UNDP Data

Mineral prospecting projects were conducted in two areas, namely Menderes Massif and Merzifon-İspir, jointly by the Government of Turkey and UNDP (United Nations Development Programme) during the period of 1970～1974. As a part of this project, a geochemical reconnaissance survey was conducted and 19,282 geochemical samples were collected from the stream sediments of the Merzifon-Ispir area (2,400km²) which includes the Gümüshane area. The sampling density was 1.2km² per one sample. In the Merzifon-İnspir area, 47 geochemical anomalies were detected on the basis of the threshold values of Cu:100ppm, Mo: 5ppm, Pb:70ppm, Zn:220ppm. There are 12 anomalies in the surveyed area excluding Zone A, and eight are believed to be promising (UNDP technical Report 2, 1974). The promising anomalous zones in the surveyed area for fiscal 1985 are shown in Figure 23 and Table 6.

Table 6 List of Geochemically Anomalous Areas Extracted by UNDP

Anomaly Area	Area(km²)	Geochemical Values (ppm)
① Beşkise	5.1	Cu:110～290(6), Mo:10～29(4), Pb:90 ～110(3)
② Arpali	6.0	Mo:29(1) Pb:70～200(5), 500(1), Zn:550,800(2)
③ Kalkanlı	114.8	Cu:110～650(19) ,Mo:10～15(3) Pb:70～250(6), 260～850(14), Zn:250～400(6),1200(2)
④ Mezraa	10.3	Cu:110～ 240(4), Pb:75～230(6), 430～1,000(2) Zn:550(1)
⑤ Karadağ	20.5	Cu:120～320(11), Mo:38(1), Pb:70～200(10) Pb:450～1,000(7), Zn:230～450(2),700～1,100(5)
⑥ Dereici	5.0	Mo:8～38(3)
⑦ Eski Gümüşhane	6.6	Cu:130～350(3), Pb:75～200(6), 300～1,300(6) Zn:250～300(4), 1,300～1,700(2)
⑧ Midi	9.7	Pb:110～700(10), Zn:2,500,3,500(2)

( ) : Number of anomalous values

The analysis by UNDP was done using only one threshold value for Merzifon-İspir area, but for a particular area, the threshold values change by the range of overlap of the distribution of the background population and the anomaly population. Thus it is necessary to clarify the distribution of the two populations and to select new threshold values.

Before conducting geochemical prospecting, we statistically processed and

re-analysed the UNDP geochemical data of our area for 1985. The elements considered were Cu, Mo, Pb and Zn which are closely related to mineralization. The number of samples were Cu 2,018 samples, Mo 1,777, Pb 1,095 and Zn 1,312.

Re-analysis was done by Lepeltier's (1969) method which will be explained later. The cumulative frequency distribution curve for all elements consists of two populations, both showing approximate lognormal distribution. They are the anomaly population and the background population. The threshold values (t) and other statistical parameters obtained from the cumulative frequency distribution are as follows.

Element	N	Mean(M)	M+σ	M+2σ	Max.value	Min.value	t	t'
Cu	2,018	32	68	144	650	1	90	100
Mo	1,777	2.2	3.6	6.0	50	1	6	5
Pb	2,095	40	96	230	1,900	3	105	70
Zn	1,312	88	171	331	3,500	9	215	220

σ : standard deviation assuming lognormality (ppm)

N:Number of Samples, t:Threshold of Surveyed Area, t':Threshold of UNDP

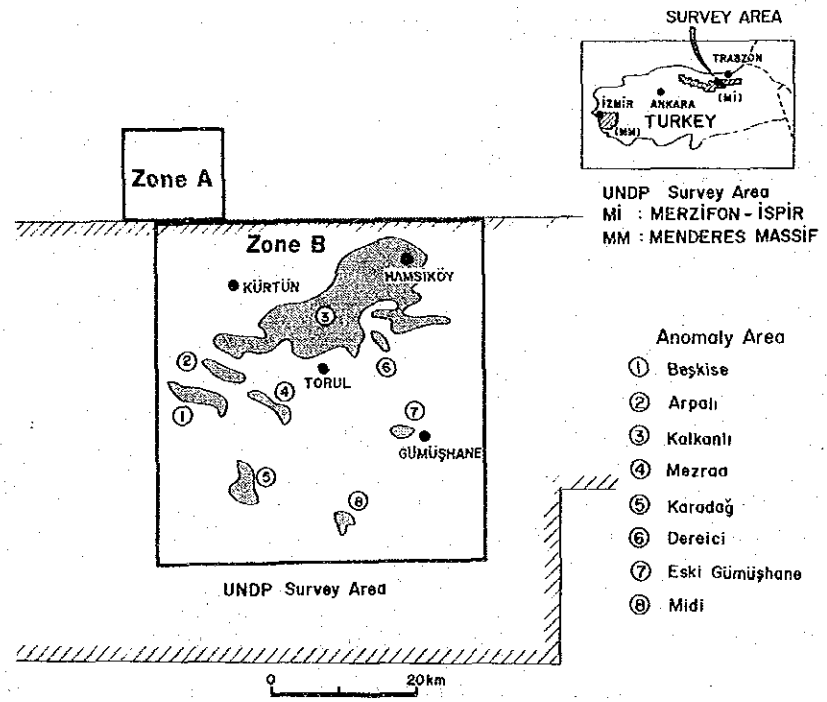

Fig.23 Geochemically Anomalous Areas Extracted by UNDP

3-2 Stream Sediment Geochemical Prospecting

Zone A: As geochemical sampling had not been carried out, sampling was done using 0.5km^2/sample and Cu, Mo, Pb, Zn, Ag indicators.

Zone B: UNDP sampled the area at 1.3km^2/sample and geochemical anomalies have been detected. Three zones with strong Cu-Mo anomalies and the area of the

Gümüshane Granite distribution were sampled. The number of collected samples was 406 in Zone A and 504 in Zone B.

Sampling density is a very important factor in assessing the population during statistical treatment of geochemical prospecting data. More than 3,000 geochemical samples have been collected including UNDP data from the surveyed area. But there are local variations of sampling density, 2 samples/km^2 in Zone A and 1.0～0.7 samples/km^2 in Zone B. As the densities are different, data should be treated separately. Considering two populations, one for Zone A and the other for Zone B, we studied whether significant differences existed between the mean values of the two populations.

All analytical data were converted to logarithmic values, mean value (M), standard deviation (σ), frequency and cumulative frequency were calculated by computer for each element together with the correlation coefficients between each element pair. The flow chart of this process is shown in Fig. 24.

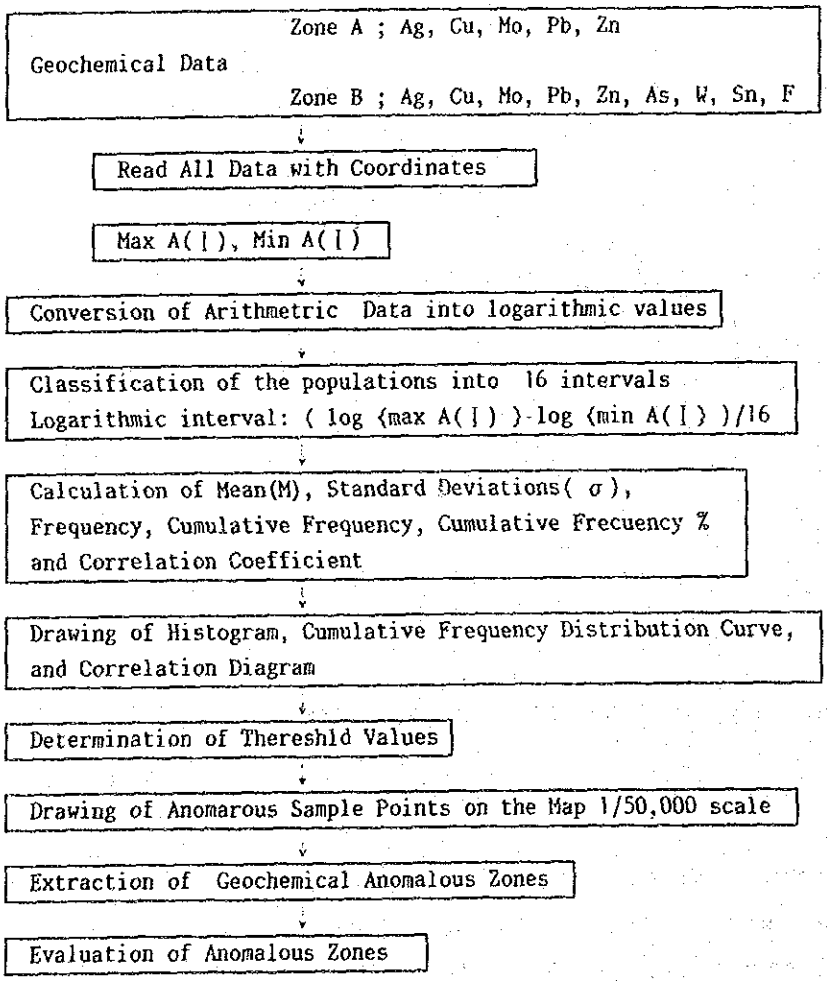

Fig. 24 Flow Chart of Statistical Treatment of Geochemical Data

Strong positive correlation is observed for Pb-Zn in both Zones A and B, with coefficicent higher than 0.7. Weak positive correlation is observed for Ag-Pb, Cu-Zn, Cu-Pb, Cu-Mo, Cu-As, Pb-As, Zn-As. As for W, Sn (Ag, Mo), they exist in most of the samples below the limit of detection and thus clear correlation is not shown. There are no element pairs with negative correlation.

The threshold values of each element were determined by C.Lepelier's (1969) method. That is, when the cumulative frequency distribution is expressed as a straight line decreasing to the right, the 2.5% point was taken as the threshold value; when the line bent at a point below 50%, the breaking point was taken; and when there were two breaking points, the mid-point between the two was used. For Ag, W, Sn, Mo, however, most values were below the limit of detection and thus frequency distribution is not clear, and $M+2\sigma$ was used as the threshold value. The cumulative frequency distribution of Cu, Pb, Zn show clear positive skewess for both zones and the values for these elements are divided into background unit groups and anomaly unit groups for both zones. For F and As, however, it became almost straight and it was not possible to distinguish the plural groups. The determined thereshold values are as follows;

	Ag	Cu	Mo	Pb	Zn	As	W	Sn	F
Zone A	0.5	174	7	154	293	-	-	-	-
Zone B	0.6	100	6	100	227	105	5	3	631

(ppm)

Anomalous zones were delineated using the threshold values for each element. The extracted zones are shown in Fig. 25. The anomalous zones are defined here as those areas where anomalies of two or more elements overlap or where two or more adjoining sampling sites show anomalous values.

There are not many anomalaus zones in the southern part of the surveyed area where Pre-Cretaceous formations are distributed, while a fair number of such zones occur in the northern part where Upper Cretaceous units are widely distributed. These zones in the north exist in large scale where combinations of andesite-limestone and intrusions of young granodiorite occur and are related to those two units. Of these zones, Kalkanlı (Anomaly zone B-11) and Der dere(Anomaly zone B-15) are elongated in a NE-SW direction and it is noted that this trend agrees with that of the young intrusive body. Also, some W, Sn, As, F anomalies were detected in the south, but most of them were for only one element and sporadic. Only a very few formed anomalous zones consisting of overlaps of more than one element.

Anomalous zones were classified into four ranks, namely A, B, C, D, by the geochemical data such as number of anomalies in the zone, the strength of the

anomalies, the number of elements which overlap, the size of the zones and the geochemical conditions of the known mineralized and alteration zones. All the delineated anomalous zones are listed in Table 9.

Table 7 Statistical Parameters of Geochemical Samples

Zone A

	N	Mean(M)	Min.Value	Max.Value	σ	M+σ	M+2σ
Ag	406	0.12	0.1	10.7	0.290	0.2	0.5
Cu	406	48.4	1	5,500	0.471	143.0	422.8
Mo	406	1.5	1	120	0.317	3.0	6.3
Pb	406	41.0	1	9,000	0.524	137	457.9
Zn	406	105.2	2	3,140	0.360	241.2	552.9

Zone B

	N	Mean(M)	Min.Value	Max.Value	σ	M+σ	M+2σ
Ag	504	0.14	0.1	6.7	0.306	0.29	0.58
Cu	2,522	30.2	1	780	0.361	69.3	159.0
Mo	2,281	2.0	1	50	0.245	3.4	6.1
Pb	2,599	38.0	1	3,250	0.395	94.5	234.8
Zn	1,816	89.2	9	3,500	0.293	175.4	344.6
As	504	12.1	1	190	0.466	35.3	103.4
W	504	1.3	1	125	0.255	2.4	4.2
Sn	504	1.1	1	18	0.142	1.5	2.1
F	504	327.5	100	1,900	0.152	464.3	658.3

(ppm)

N: Number of Samples, σ : Standard deviation, assuming lognormality

Table 8 Correlation Coefficients for Trace Elememts of Stream Sediments

Znea A

	Ag	Cu	Mo	Pb
Cu	0.433			
Mo	0.430	0.424		
Pb	0.500	0.364	0.325	
Zn	0.452	0.605	0.273	0.727

Zone B

	Ag	Cu	Mo	Pb	Zn	As	W	Sn
Cu	0.404							
Mo	0.181	0.430						
Pb	0.622	0.540	0.165					
Zn	0.514	0.555	0.104	0.739				
As	0.456	0.437	-0.029	0.573	0.536			
W	0.092	0.013	0.164	0.041	0.028	-0.022		
Sn	0.090	-0.144	-0.055	-0.039	-0.038	-0.083	0.138	
F	0.108	-0.092	0.014	0.068	0.026	0.242	0.143	0.076

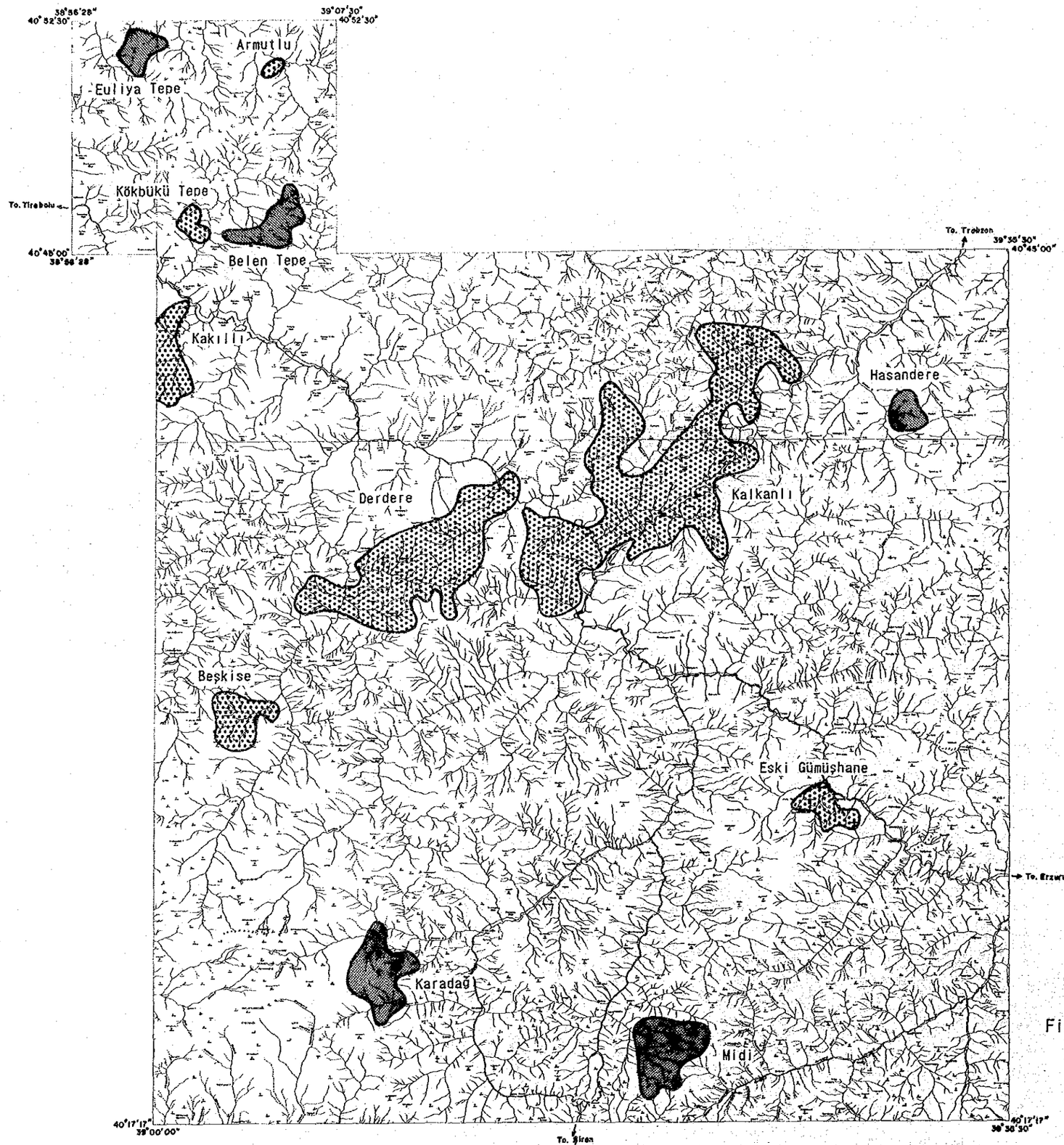

Fig. 25 Remarkable Geochemical Anomalous Areas in the Project Area

Table 9 List of Geochemically Anomalous Areas in the Project Areas

No	Name of Anomaly	Area (km^2)	Am of An Po	Range of Anomalous Values ※1 (ppm) Cu	Mo	Pb	Zn	Other elem	Geological enviroments and Related mineral occurences※2	Rank of※3 evaluation
A-1	Evliya Tepe	5.5	10	245～600(5)	9～12(3)	1,500-2,800(5) 350-860(4)	1,060-3,140(4) 610-830(2)	Ag 0.5-3.9(6) Ag 6.3-10.7(2)	Kzl, Kza2, qp: Aşağı Sıgırlık Mine (vein,skarn Cp-Py-Gn-Spec)	A
A-2	Armutlu	1.1	2	770(1)	9, 42(2)	160, 205(2)	1,020(1)	-	Kzdl, Kza2: Armutlu altered zone (sili, limo.Py-Cp-Oxcp)	B
A-3	Gecür	1.4	3	190 455(2)	9, 19(2)	180(1)	-	-	Kzdl, Kza2	C
A-4	Gırlak	1.8	3	1,000 175(2)	7, 17(2)	-	-	-	Kza2, gd: Gırlak (Skarn, Spec, Oxcp)	C
A-5	Kurtbeli Dere	1.2	2	210(1)	-	330(1)	295, 305(2)	-	Kzdl, gd: argillized tuff	D
A-6	South of Büyük Tepe	2.3	1	-	-	185(1)		Ag: 1.1(1)	Kza2, Kzd2: week silicification, Py-diss in D2	D
A-7	Keltaş Tepe	1.3	3	-	-	360-420(3)	467～490(2)	-	Kzd2: Keltaş güney Mine (vein, Py-Cp)	D
A-8	Belen Tepe	6.5	9	270～620(5) 1,640(1) 5,400(1)	10-19(4)	210-420(2) 9,000(1)	320～590(5) 2,270(1)	Ag 1.2-2.4(3)	Kzl, Kza2, gd: Dere and Kuru Mines (Skarn, Cp-Gn-Py-Spec)	A
A-9	Kökbükü Tepe	2.1	4	960(1) 360(1)	7(1) 120(1)	-	-	Ag 0.6(1)	Kzdl, Kza2: week Py-diss	B
B-1	Mindizli	3	3	164,197(2)	-	249(1) 527～1,320(4)	319(1 430～760(4)		gd(kürtün body) Kza1, Kzdl	D
B-2	Nabaşa	20	16	117～296(4)	6(1)	100～435(12)	230～390(8)		Erikbeli Yayla altered zone (Py-diss)	C
B-3	Konacık	3.6	2	440(1)	6(1)	202(1) 530(1)	1,140(1)	-		C
B-4	Düzköy	6	4	140～234(4)	6(1)	115(1)	-	-	Kzl, Kza1, gd: Düzköy (skarn, Spec-Cp-Py-Gn)	C
B-5	Kakıllı	11	9	229(1)	6～10(5) 40～50(3)	110～140(5)	250(1)	-	gd	B
B-6	Dikme Tepe	6.5	7	-	-	102～280(6) 475(1)	230～246(2) 545～685(2)	-	Kza1, Kzl, Kzdl, gd: Çatak and Kurtukluyurt (Skarn, Spec-Mag)	C
B-7	Ziyaret Tepe	4	3	115(1)	-	381～442(2)	425～444(2)	-	Kza1	C
B-8	Dolumlu	1.7	2	147,320(2)	-	-	-	-	Kza1 Dolumlu (Skarn, Spec-Py-Oxcp)	D
B-9	Kızılağaç Yayla	0.5	1	180(1)	10(1)	-	-	-	Kza1, gd	D
B-10	İstala	2.3	3	109(1)	-	100～260(3)	240,290(2)	-	Kza1	D
B-11	Kalkanlı	103	110	400～650(10) 240～332(6) 100～200(30)	9～15(6) 28(1)	750～3,250(7) 300～606(17) 100～297(73)	1,000～1,560(4) 400～650(15) 230～385(32)	Ag 0.6～2.0(10) As 110～180(4) F 770(1)	Kza1, Kzdl, Kza2, gd: Köstere, Istala Mines Şive, Kalkanlı, Köstere and other altered zones	B
B-12	East of Büyükdüz Tepe	6.3	3	111, 186(2)	-	129, 174(2)	240,290(2)	-	Kza1, Kzdl, gd: silicification with Py	D
B-13	Araköy Yayla	3.2	3	-	6(1)	-	228(2) 520	-	Kza1, Kzdl,gd: silicification with Py	D
B-14	Mandıra	0.5	1	159(1)	6(1)	110(1)	-	-	Kza1	D
B-15	Derdere (Herek)	39.5	33	104～125(3)	6～15(3)	500～900(9) 300～450(7) 120～298(15)	291～550(4)	-	Kza1, gd: Herek altered zone(sil.and arg.with Py-Cp-Gn-Sph)	B
B-16	Sarısaman	2.5	6	-	6～10(5)	-	-	W 6, 9(2)	gd: silicification and limonitization	C
B-17	Hasandere	5.3	8	780(1) 182～346(7)	14～28(4) 8～10(2)	222(1)	600, 685(2) 293(1)	W 7～13(4) Sn 5(1) Ag 0.6-1.4(2)	Kza1, pg1, pg2: Hasandere mineralized zone (Py-Cp-Mo stockworks)	A
B-18	Bakımlı Yayla	4.5	4	107,110(2)	6(1)	105～150(3)	-	-	Kza1, pg2	D
B-19	Derindere	5.7	5	100～110(3)	-	114～290(5)	256(1)	-	Kza1	D
B-20	İstavri Dere	8.5	7	100～220(4)	-	100～190(4)	-	W 125(1)	Kza1, gd: silicification and limonitization with Py	D
B-21	Köydere (Torul)	3.2	5	100, 130(2)	6～10(4)	-	-	W 9(1) F 890(1)	Kza1,gd silicifi. and argilli.	D
B-22	Tüfekçili	0.7	1	-	-	245(1)	239(1)	-	Kzl,Kza1,qp,gd	D
B-23	Görükse	1.8	2	-	29(1)	196,200(2)	268,850(2)	-	Kza1,gd	C
B-24	West of Makrelbaşı Tepe	1.2	1	-	-	500(1)	550(1)	-	Kza1,gd	D
B-25	Çamdibi	3.5	3	120(1)	-	1,000(1) 120,230(2)	550(1)	-	Tva,Jkb Qz vein with Cp,Oxcp	C
B-26	Beşkise	12	19	320～480(5) 219～265(4) 100～107(4)	26 (1) 13～18(3) 6～9(7)	110～160(4)	-	-	Kza1, gd: Beşkise altered zone(Sil., limo.with py)	B
B-27	Otalan	7.5	9	100～140(6)	6～11(3)	100～110(4)	230～245(3)	-	Kza1, gd: Otalan altered zone(Sil., limo.with py)	C
B-28	Kopuz	0.9	1	-	-	265(1)	740(1)	-	Kza1,gd	D
B-29	Avlıyana	2.3	2	122(1)	10(1)	-	-	-	Kzf, Kza1,gd	D
B-30	South of Haviyana	2.3	2	110,120(2)	-	450(1) 1,000(2)	-	-	Tva,Kzf,gd	D
B-31	Zaimli	1.3	2	-	-	100(1)	-	-	Jkb,Jkul	C
B-32	Soğuksu	0.8	2		18(1)	200(2)	-	-	Jkb,Jkul	D
B-33	Eski Gümüşhane	5.7	14	130～350(4)	-	750～1300(4) 252～510(3) 150～220(5)	950～2400(6) 300(2)	6.7(1) 0.6～0.9(2) Sn 3(1)	Jkb, Jkul, Pgg, gd.: Kırkpavli(Au,Ag),Hazine Mağara (Ag, Gn, Sph, Cp,Tet)	B
B-34	Karamustafa	2.8	2	-	-	-	-	W 8,14(2)	Pgg:	D
B-35	Işik	0.6	2	110, 205(2)	-	110,145(2)	230,265(2)	-	Pgg:	D
B-36	Manador Tepe	7.5	4	120(1)	38(1)	350(1)	-	W 8(1) As 113(1) F 640(1)	Jkb, Pgg, Kza1,gd:	C
B-37	Karadağ	10.8	16	120～180(6)	210～340(7) 8(1)	1,600～2,100(4) 450～800(8)	700～1,060(6) 230～450(3) 200(2)	Ag 0.8～2.4(4) W 9(1)	Kzl,Kza1,qp,gd: Karadağ Mine (Skarn,Cp-Gn,Sph-Spec)	A
B-38	Altıntaşlar	2.4	5	100(2)	-	220～475(4)	240～400(3)	Ag 0.7～0.9(2)	Jkd,Pgg,gd Altıntşlar mineralized zone (cp-py)	C
B-39	Hatipler	0.6	1	110(1)	-	260(1)	-	-	Jkb,Pgg	D
B-40	Midi	11.2	14	-	6(3)	336～780(4) 110～150(9)	2,500～3,500(3) 228～400(3)	Ag 0.6,2.3(2) As 170(1) Sn 4,18(2)	Jkb,Pgg Midi Mine vein(Sph-Gn)	A
-41	North of Tozlu Tepe	5.6	5	-	-	-	-	W 7～21(4)	Pgg:	C

※ 1 Figures in parentheses are amount of anomalous samples.
※ 2 See abbreviations in Fig.7
※ 3 Priority: A, B, C, D, in order.

Part 3 GÜZELYAYLA AREA

Part 3 GÜZELYAYLA AREA

Chapter 1 Geology and Mineralization

1-1 General Geology

The geology of the Güzelyayla Area is divided roughly into the Jurassic Kırıklı Formation, the Kuşakkaya Limestone Formation and the Upper Cretaceous Zigana Formation. The Zigana Formation is further divided into five stratigraphic units-namely the Kermutdere, A1, D1, A2 and D2 Members in ascending order as determined by the first phase survey, but only the A1 Member of lowest Zigana Formation is distributed in the surveyed area. Porphyritic granite and quartz porphyry have intruded into the formations, and small andesite and basalt dykes are observed in the area.

Porphyritic granite is classified into two types, namely altered porpyrytic granite having a close relationship with mineralization and unaltered porphyritic granite having no association with mineralization. The former type is a small rock body distributed around Hasan Dere, while the latter type forms a rock body elongated in the ENE-WSW direction

The geological map, geological profile maps and schematic geological column are shown respectively in Figs. 26～28.

1-2 Stratigraphy

Kırıklı Formation : This formation is distributed from the north west part to around Hamsiköy in the surveyed area, and consists of basaltic lava and basaltic pyroclastic rock. At the north-western part of the surveyed area, only basaltic lava is exposed in small range This rock is a dark green to reddish brown finely grained massive, and has undergone strong chloritization and epidotization. Amygdaloidal texture is microscopically common, and plagioclase is chloritized.

Kuşakkaya Limestone Formation : This formation consists of massive limestone, and its distribution is limited to a locality downstream of the Kiraz Dere. However, it is widely distributed around Dikkaya Village in the northern part of the surveyed area, overlying the Kırıklı Formation. The limestone of this formation is grayish white to white and mostly massive with no bedding. Downstream of the Kiraz Dere, this limestone has been altered to crystalized

limestone owing to thermal metamorphism by intrusion of porphyritic granite, but is not accompanied by sulphide ores. As will be mentioned later, this limestone lies in fault contact with the Zigana Formation, which is the upper formation, and consists of altered andesite accompanied by sulphide ores.

Zigana Formation : This formation has been divided into the Kermutdere, A1, D1, A2, D2 Members in ascending order, but only the A1 Member is widely distributed in the surveyed area. This member consists of andesitic lava, andesitic pyroclastic rocks and thin beds of limestone and siltstone.

Andesitic lava : This rock is a pale green to dark green massive or hyaloclastic basaltic andesite. The rock has been brecciated owing to hyaloclasts, and consists of breccia and matrix of the same material incorporating subangular pebbles of limestone and siltstone. Hyaloclastic basalt changes laterally to a massive lava rock facies. At the fault boundary, running in a north-south direction in the western part of the surveyed area, a remarkable difference in alteration mode is observed. The rock has undergone strong alteration and has developed many cracks and fissures caused by an intrusion on the east side of the fault, whereas weak alteration with only chloritization and epidotization occur on the west side of the fault. This alteration, as will be mentioned later, is sericitization and chloritization distributed around porphyry granite (Pg1). Chalcopyrite-molybdenite-pyrite bearing mineralization is observed along fissures and quartz veins in cliffs at Maden River or in rock exposures by the forest road. It is very difficult to microscopically identify the rock in this part because of strong alteration.

Andesitic tuff : Well-bedded andesitic tuff is partly intercalated in andesite lava. The tuff is a pale green to reddish green coarse grained rock. The rock may be a member of the hyaloclastite, as it is discontinuous and gradually changes to hyaloclastic lava.

Siltstone-sandstone and limestone : These rocks are intercalated as thin discontinous beds in the andesite lava. Thick, well-bedded alternating beds of siltstone and sandstone are distributed at Kirazbası Mountain in the eastern section of the surveyed area. The limestone is poor, discontinuous, and grades into a siltstone-sandstone bed in the same horizon. It is partly altered to crystalline limestone.

Intrusive Rocks : The main intrusive rocks are porphyritic rock and quartz porphyry with distributions of small andesite and basalt dykes. Porphyritic granite and quartz porphyry are, respectively, classified into two types based on alteration modes.

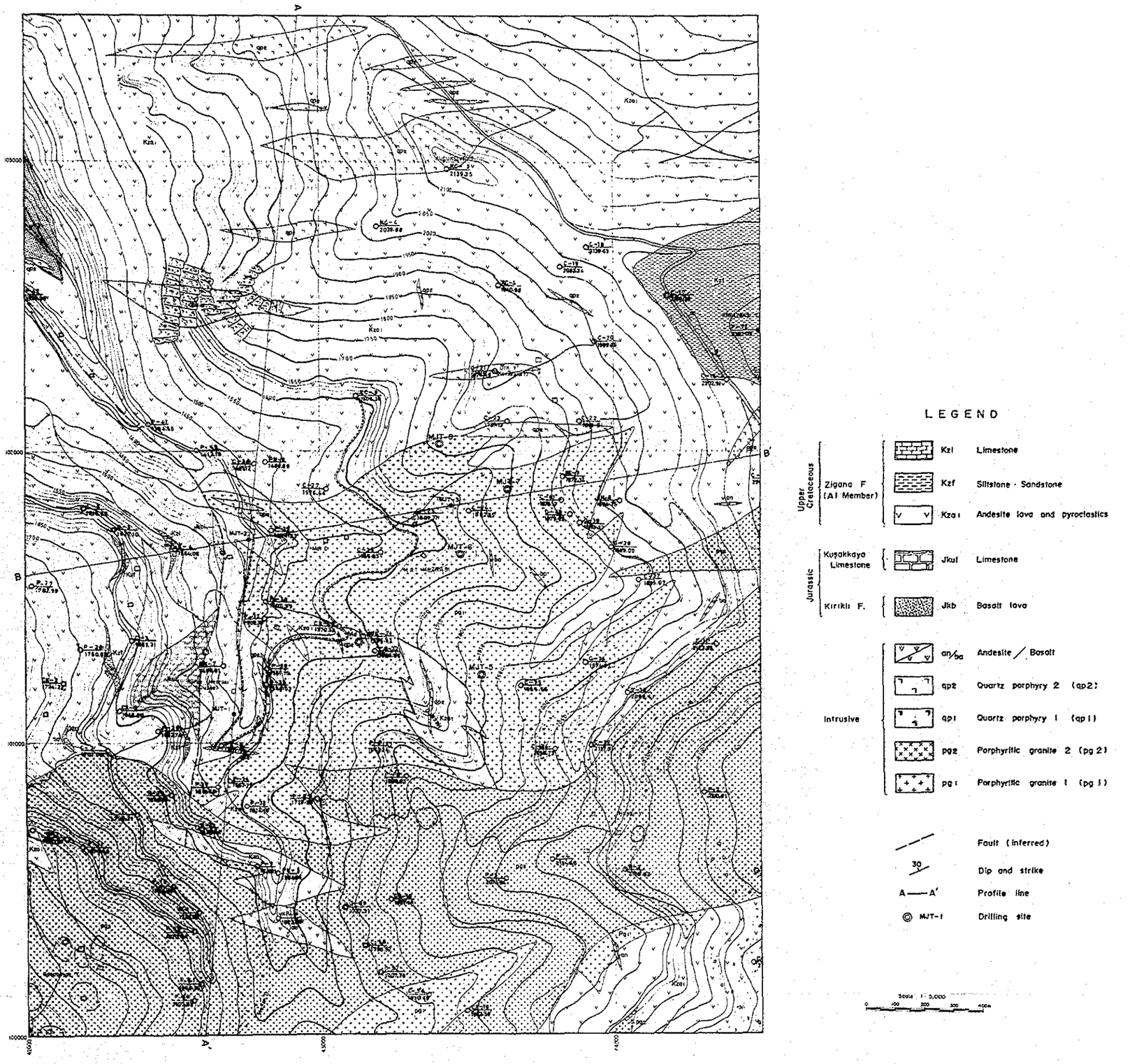

Fig. 26 Geological Map of the Güzelyayla Area

A — A′

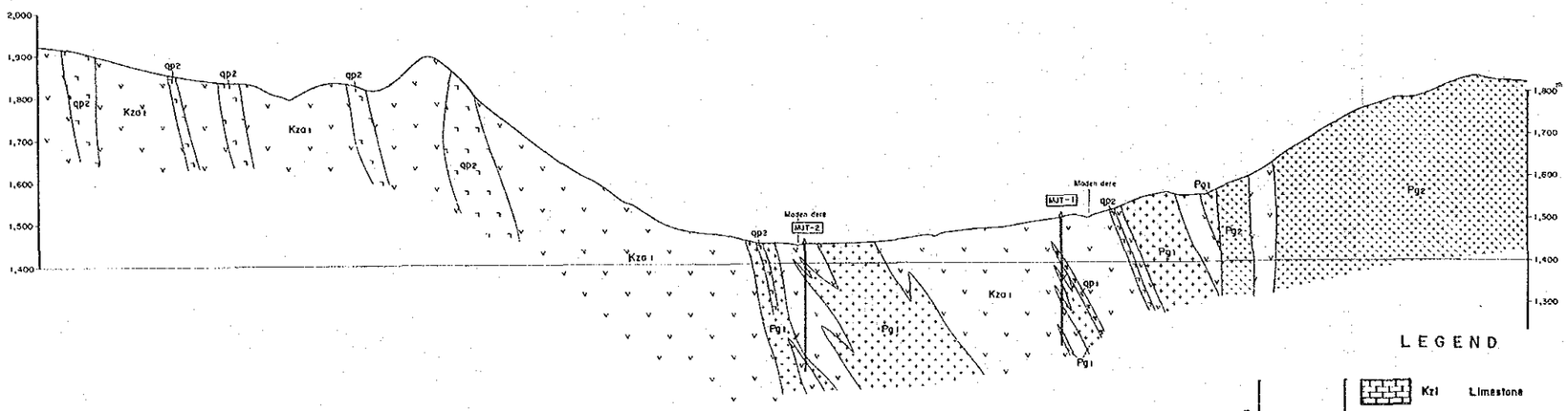

B — B′

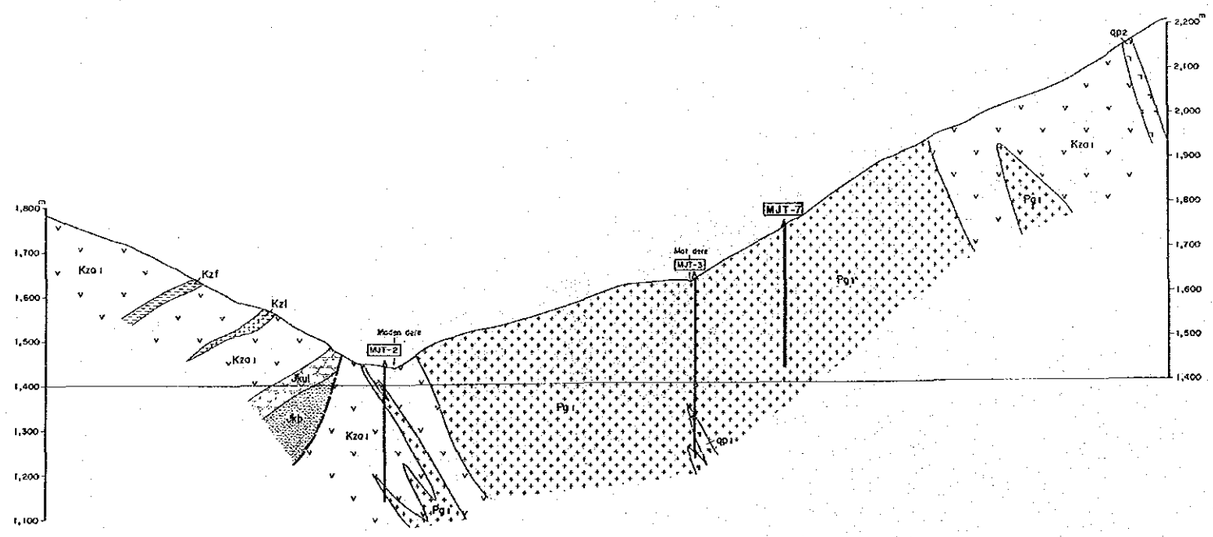

LEGEND

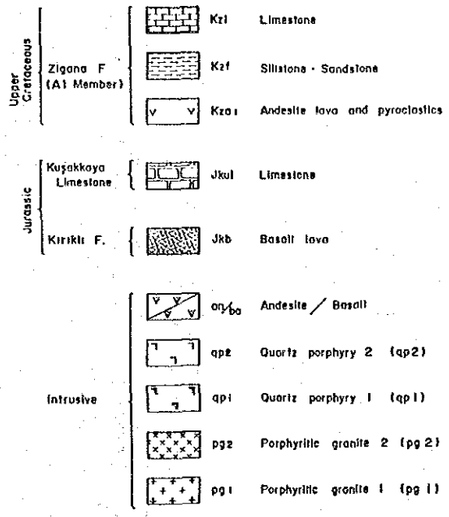

Fig.27 Geological Profile Maps of the Güzelyayla Area

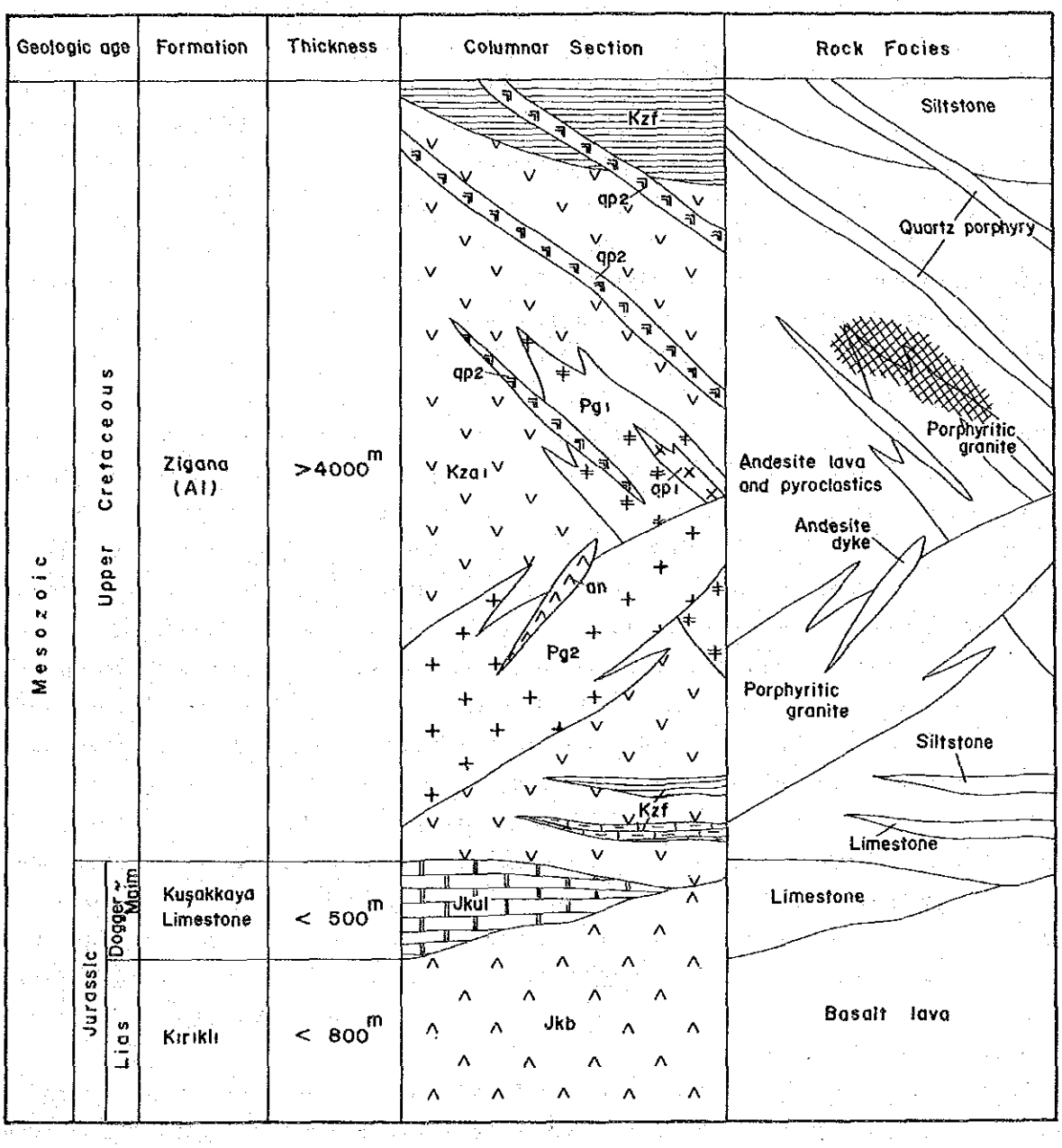

Fig. 28 Schematic Geological Column of the Güzelyayla Area

Altered porphyry granite (Pg1) : This rock is distributed in the range of about 1.5 km north-south and about 1.5 km east-west, centered in the area of Hasan Dere and Mat Dere, and is embedded in the andesite of the Zigana Formation. Porphyritic texture of quartz and feldspar is common in the rock, and facies of the rock are similar to those of the unaltered porphyry granite (Pg2, below), but the rock is easily discriminated by noting that Pg1 has undergone strong silicification and argillization consisting of sericite and biotite. Mineralizations of pyrite, chalcopyrite and molybdenite are embedded along fissures and quartz veins at Hasan Dere. Porphyritic granite, which has been altered to white rock accompanied by disseminations of pyrite, is partly distributed at the southern part of the surveyed area. Porphyritic granite ranges microscopically from a diorite facies to a granodiorite porphyry facies with porphyritic texture. Alteration and mineralization occurring in the quartz diorite rock are weaker than in others under microscopic observation.

Unaltered porphyritic granite (Pg2) : This occurs as a large batholitic rock elongated in an ENE-WSW direction and is widely distributed at Turnagol. This rock is pale green to grayish and commonly contains porphyritic texture consisting of quartz and plagioclase. Some of the mafic minerals are altered to chlorite and epidote, but generally, the rock has undergone little alteration. It may be inferred that Pg2 is a later intrusion than Pg1, because the former, found close to the latter in the field, is substantially free of alteration by mineralization, although a chronological relationship between the two intrusions was not observed in the field. Although the litholgy of MJT-6 consists of Pg1 and Pg2, the relation between both porphyritic granites could not be clarified because of well-developed crushed cores. The rock is holocrystalline with a porphyritic texture, and alteration of biotite and hornblende to chlorite, epidote, sericite, and calcite can be seen through the microscope.

Quartz porphyry (Qp1) : The existence of this rock body was confirmed by MJT-1 and MJT-3. This rock has intruded into andesite of the Zigana Formation at MJT-1, and into Pg1 at MJT-3. Both host rocks have undergone sericitization and silicification, and chalcopyrite and molybdenite are embedded along fissures and quartz veins in the rock.

Quartz porphyry (Qp2) : This rock is found around Kücüksivrı Mountain and at Maden River, and has intruded into andesite lava, and partly into the altered porphyritic granite (Pg1). It is inferred that the intrusion activity of the quartz porphyry (Qp2) is later than that of Pg1 due to the relationship between both rocks as mentioned above.

Andesite dyke (an) : A dark green massive andesite dyke is observed at the conjunction of Maden and Saralim Deres. This dyke cuts the andesite of the Zigana Formation and Pg2 in a WNW-ESE direction. There are also other small

dykes up the Mat Dere cutting Pg1 and the andesite of the Zigana Formation. This rock is porphyritic in texture, and the constituent minerals of plagioclase, hornblende, and pyroxene have been replaced by chlorite and calcite through weak alteration as seen under microscopic observation. The rock is named quartz bearing andesite.

Basalt dyke (ba) : Narrow basalt dykes several meters in width are observed at four places up the Mat Dere and MJT-6. These dykes have varying strike directions (N-S, NE-SW, NW-SE, etc.) at Mat Dere. Pg1 was intruded by basalt from 289m to 298.40m (real width;7～8m) at MJT-6. The basaltic rock has an interstital texture, and plagioclase, biotite and hornblende of the constituent minerals are slightly altered to chlorite and calcite in thin section.

1-3 Geological Structure

The surveyed area is situated on the wing of an anticlinal structure extending N-S to NE-SW from Hamsiköy to Dikkaya. The geological structure of the area is largly controlled by this anticlinal structure, but some structural disturbances owing to the effects of the porphyritic granite intrusion from the central to western part of the surveyed area and of the subsequent fault activity occur. The Zigana Formation dips westward on the west side of the fault and northward or eastward on the east side of the fault. The fault, thought to be running along the east side of Maden Dere in a N-S directional system, extends northward out of the surveyed area, while it disminishes at the southern extention as it is cut off by the intrusion of Pg1. Displacement by the fault has raised the western side, judging from 1) the distribution of the Kuşakkaya Limestone formation, which is a lower Formation than the Zigana Formation, and 2) the absence of Mo-Cu mineralization or minera-lized alteration on the west side of the fault. The quartz porphyry extends in an east-west direction, differing from the north-south system of the fault.

1-4 Mineralization and Alteration

The mineralized zone is embedded in Pg1 and in the andesite of the Zigana Formation in the vicinity of the granite in an area from Mat Dere to Hasan Dere which are tributaries of the Maden River, situated 4 km south-east of Hamsiköy.

As mentioned before, the porphyritic granite consists of Pg1 accompanied by Mo-Cu mineralization along fine fissures and of Pg2 with very weak alteration without mineralization.

Observed with the naked eye, both porphyritic granites resemble their rock facies, but intruded at sightly different times. The former intruded earlier in a confined area while the latter is exposed south of the former and extends NE-SW.

The mineralized zone is characterized by molybdenite-chalcopyrite-pyrite mineralization emplaced along fine fissures caused by the Pgl intrusion and consists of the following parts:

① those embedded along fissures with quartz veins (vein type)

② those embedded as filmy veinlets (fissure type)

③ those embedded as disseminations (dissemination type)

Vein and fissure type mineralizations are common at Maden, Mat, and Hasan Deres, but mineralization on the ridge of the mountain, being topographically high, is strongly limonitized owing to the effects of rain and snow. Also, due to forest cover, the above mentioned characteristics of mineralization were not observable. In such areas, copper was leached, and surface soil usually contained very low grades of Cu, as seen in the results of the soil geochemical survey, but there is a secondary enrichment zone 1m～10m below the surface.

In MJT-1 and MJT-2 of the drilling survey located in Maden Dere, vein and fissure types are continuously observed from ground surface to 301m. Conversely in MJT-3 to MJT-8, located on convex topography, dissemination type is dominant, accompanied by vein and fissure types, except in a section of secondary enrichment consisting of native copper, chalcocite and covelline in fissures and as diseminations from surface to 120 m in depth.

The ore minerals are mainly pyrite, and some chalcopyrite and molybdenite. Chalcocite was found in a boulder at Mat Dere, and malachite along Mat Dere, but no molybdenite was observed at Mat Dere in the area of the Mo geochemical anomaly detected by the soil geochemical survey of the initial phase. Minor amounts of native copper, covelline, galena, sphalerite, magnetite and hematite are observed in drill cores. Pyrite is embedded as disseminations, networks and veins and is associated with other sulphide ores. It occurs throughout the long mineralization stage, from early stages to later stages. Most chalcopyrites co-exist with pyrite along fissures, and is cut by molybdenite-pyrite-quartz veins. This is predominant in MJT-2, but chalcopyrite-pyrite veins exist along fissures of chalcopyrite-pyrite in the disseminated section.

Under microscopic observation, chalcopyrite-pyrite cuts aggregated magnetite. Therefore, paragenesis of ore minerals is: magnetite was crystallized in the first stage, chalcopyrite-pyrite followed magnetite, and molybdenite-quartz occurred, filling in cracks (cavities) around pyrite crystals at a later stage. Very minor amounts of sphalerite may have crystalized with chalcopyrite, since they exist together in exsolution texture.

This fact observed through the microscope reveals that these ore minerals might have crystallized in the following order: magnetite→pyrite→chalcopyrite • sphalerite→molybdenite. This relationship is consistent with field observations. The mineralized zone in the Pg1 intrusion is expected in an area of diameter 1.8km～2.0km. The area is delineated by Cu anomalous values of more than M+σ (200ppm), and centers around a high Mo anomalous zone, as found by the geochemical survey conducted by MTA. It covers the stock intrusion of Pg1 and the surrounding andesite intruded by Pg1.

Chip samples for investigation of the chemical constitution of the ore were collected in the Hasandere Area in which mineralized showings of porphyry copper type are recognized. The assay results indicate that copper exposed on the ground surface was leached owing to much precipitation of rain and snow, and shows very low grade. Molybdenum content values of these samples are also low grade except for samples from the Mo geochemically anomalous area. These chip sample results are of lower grade than that of drill core. The leached nature of the chip samples may be the cause of this discrepancy. Good correlation between Cu and Mo values of the chip samples is not recognizable as is the case with the soil geochemical survey.

Samples for X-ray diffraction analysis were collected in the area of the Pg1 stock and surrounding andesite at Maden, Mat and Hasan Deres in order to unravel the zoning of alteration by mineralization. The result was compiled in the map of alteration zoning. Together with microscopic observations of thin sections, the alteration zoning map of ground surface is in Fig.29. Samples for X-ray diffraction analysis were collected from MJT-1 to MJT-8. The alteration zoning map of drill core is in Fig.30.

Altered clay minerals detected through X-ray diffraction analysis are mostly sericite and chlorite with additional kaoline, pyrophylite, montmorillonite and mixed-layer mineral. Core samples located at the periphery of the potassic zone contain chlorite and sericite. In this zone, sericite rich white rock is classified into the phyllic zone, while chlorite rich greenish rock is classified into the propylitic zone. The outer parts of the phyllic zone, chlorite rich propylitic zone, and further outer zones tend to decrease in chlorite content while increasing in epidote content. Pyrophyllite and kaoline also occur locally at the southern end of the Pg1 stock which has been intruded by Pg2.

This pattern of alteration zoning is similar to the Lowell-Guilbert model (1970) of potassic zone → phyllic zone → propylitic zone outwards from the core. In the case of this surveyed area, the outer limit of the propylitic zone was delineated as an area of 1.8 km× 1.8 km, on the basis of the anomalous area of Cu and Mo as found by the soil geochemical survey conducted by MTA.

Chapter 2 Fliud Inclusions

2-1 Measurement of Fluid Inclusions

Samples for measuring fluid inclusions were collected in the Hasandere area in which promising porphyry copper ore deposit is expected. Samples were collected from the following rocks, and their amounts are as follows :

(1) Altered porphyritic granite(Pg1)	90 samples
(2) Unaltered porphyritic granite(Pg2)	15 samples
(3) Quartz porphyry(Qp1)	3 samples
(4) Andesite(Zigana Formation)	42 samples
Total	150 samples

Among these samples, quartz veins and quartz phenocrysts were from the altered porphyritic granite(Pg1) (regarded as the ore-bringer intrusion), quartz phenocrysts from the unaltered porphyritic granite(Pg2) (slightly post-intrusion of Pg1) and porphyry (Qp1), and quartz veins in andesite intruded by Pg1, Pg2 and Qp1 were collected for fluid inclusion measurements.

2,719 fluid inclusions were measured from 150 samples collected. Measured fluid inclusions per sample ranged from 10 to 21 inclusions (average: 18 inclusion per sample). The number of measurements for each rock type and quartz samples are shown as follows:

	Phenocryst	Quartz vein	Total
Altered porphyritic granite(Pg1)	695 pcs	974 pcs	1,669 pcs
Unaltered porphyritic granite(Pg2)	163 pcs	82 pcs	245 pcs
Quartz porphyry(Qp1)	55 pcs	-	55 pcs
Andesite(Zigana Formation)		750 pcs	750 pcs
Total	913 pcs	1,806 pcs	2,719 pcs

As a result of the measurements, all homogenization temperatures range broadly between 250℃ and 660℃, but 90% of these values are included within the range of 350℃ to 450℃. Over 80% of the homogenization temperature values per sample are in the temperature range of 50℃ to 100℃, showing normal distribution. Such a tendency is more predominant in the quartz vein than in the quartz phenocryst.

The measurable diameter of fluid inclusions is 20μ to 30μ, but sometimes

fluid inclusions 10μ or several 10'sμ in diameter were also measured. Thin sections less than 0.3mm to 0.4mm in thickness, with both planes polished were prepared. Many fluid inclusions are surrounding by transpearent quartz . There are many inclusions less than 10μ in diameter and are elipsoidal in form. Among these inclusions, negative quartz crystal are also observed, and pseudo secondary or secondary inclusions are of irregular form.

The 2,719 pieces of fluid inclusions measured are divided into 2,315 pieces of liquid and 404 pieces of gaseous fluid inclusions. Homogenization temperature of the gaseous fluid inclusions is higher than that of liquid fluid inclusions, regardless of whether they are in rock, quartz vein or quartz phenocryst. Most fluid inclusions in the quartz vein and quartz phenocryst can be described as follows:

① Consisting of two phase inclusions (gaseous and liquid phases)

② Many liquid phase fluid inclusions usually contain carbon dioxide

③ A few solid phase inclusions are observable. Some solid phase inclusions disappear near 260℃, and others is disappear at a range of 260℃ to 620℃. The former may be NaCl crystalized tetrahegonally and the latter are somewhat round in shape but are of rather irregular form.

④ Minor amounts of polyphase inclusions are present.

⑤ Most fluid inclusions are generally tiny, namely smaller than 20 microns in size.

The mean value of homogenization temperature is 396℃ in the quartz vein of Pg1, and 388℃ in the quartz vein in andesite. It is 393℃ for total samples of both rocks. The mean value of those in quartz phenocrysts is 393℃, close to the value for quartz vein of Pg1. It is made clear, as shown in Table 13, that the difference between the mean values is statistically insignificant.

Homogenization temperatures of quartz veins from Pg1 are highest (413℃) at the Hasandere Area (MJT-5), 409℃ at Mat Dere, and 375℃ at Maden Dere; that is, the temperature decreases towards the periphery of the Pg1 intrusion. The temperature of fluid inclusions in Pg1 at the southern part where it has been intruded by Pg2 drops further to 303℃. Here there is no quartz vein and only five quartz phenocrysts were used for the measurment of fluid inclusions, in contrast with 23 quartz phenocrysts of Pg1. Therefore, it is very difficult to compare the results of both rocks. However it is roughly stated that the mean temperature of inclusion in Pg2 (348℃) is 50℃ lower than that of Pg1 (392℃).

Fluid inclusions in the quartz phenocryst of Pg2 is characterized by their small size, while that of Pg1 is somewhat larger in size, in comparison with both rocks. Solid-like inclusions which disappear at 590℃ and reappear at 390℃ such as those in AE-54 of Pg2 as well as those in YY-12 of Pg2 which disappear at 620℃ are recognized among the inclusions in quartz phenocryst.

In comparing homogenization temperatures of fluid inclusions in quartz veins in each part of Pgl, the temperature is highest (408℃) at around Mat Dere, 391℃ at Maden Dere, and tends to decline with a gentle temperature gradient. The temperature of quartz veins in andesite has the same tendency-highest(406℃) at the molybdenum anomalous area of north Mat Dere, 384℃ at Hasan Dere, and 377℃ at Mat Dere.

Solid-phase-like and gaseous fluid inclusions are characteristically observed in samples of Maden, Mat and Hasan Deres. Samples from Mat Dere contain many gaseous phase inclusions and their homogenization temperatures are usually high, as is consistant with the abovementioned pattern.

The number of fluid inclusions measured in quartz veins constituted more than 66 percent of total measured inclusions. In order to find the relationship between these fluid inclusions and their mineralization types, the quartz veins were classified into barren quartz, pyrite bearing quartz, chalcopyrite bearing quartz, and molybdenum bearing quartz. The mean homogenization temperature of inclusions was then calculated for each quartz vein type with results, as shown in the following table ;

	F.I.	Pcs	Homogenization Temperature	
			Range(℃)	Average(℃)
Barren quartz	Liq.p	209	300～560	386
	Gas.p	40	370～550	441
Pyrite-quartz	Liq.p	228	280～520	374
	Gas.p	21	380～480	421
Chalcopyrite-quartz	Liq.p	132	320～500	390
	Gas.p	25	380～500	414
Molybdenite-quartz	Liq.p	384	250～580	385
	Gas.p	47	360～560	440

The results indicate that homogenization temperature of gaseous inclusions is generally higher than that of liquid phase inclusions. Although differences between the temperatures of gaseous and liquid inclusions of each sulphide mineral type is not especially remarkable, it may be inferred that chalcopyrite was crystalized at the highest temperature conditions in the early stage, and molybdenite was succesively formed at high temperature in the gaseous phase.

As seen in the tables above,the homogenization temparature in MJT-1 gradually increases with increasing depth. Although some irregularities occur, holes MJT-2 to MJT-8 also show an overall increase in temperature with depth.

2-2 Salinity in the Fluid Inclusion

The number of measurable samples were 103 pieces among 150 samples collected, since there were mostly small inclusions and it was very difficult to observe the phase variation at the melting time of frozen inclusions owing to poor liquid phase inclusions. The result of the measurement indicates that their melting points range from from -7℃ to -17℃, and their NaCl equivalent concentration values were calculated as 4.8 wt% to 20.60 wt % through the H_2O-NaCl diagram.

The NaCl concentration values of inclusion and homogenization temperatures are, comparatively, in the definite range from 10 wt % to 15 wt %, and from 350 ℃ to 400 ℃ in quartz veins, while those values in intrusive rocks, especially in Pg1, are more dispersed. Relationship between the homogenization temperature and the salinity is shown in Fig. 31. The relationship indicates the following:

① The homogenization temperatures of most fluid inclusions are proportionally higher in salinity with higher concentration..

② The fluid inclusion in drill core contains slightly higher salinity concentration than that in quartz vein of andesite.

③ In the case of Pg1, the salinity is of higher concentration in the area of Hasan and Mat Deres, but is comparatively lower in concentration in the Maden Dere, corresponding with homogenization temperature.

In a solid phase inclusion, hydrohalite usually occurs, but it is difficult to identify the hydrohalite in this area, because the fluid inclusions are very small in size. In the case of simple crystal solid inclusions accompanied by NaCl and KCl crystals, salinity of the inclusion is detected by volume of solid and liquid in inclusion and calculation of compositions of crystal salt and soluted salt (Takenouchi 1962). Salinity values calculated by this method are higher than measurement values of solid fluid inclusions.

KCl may not be present because no solid inclusion disappeared in low temperature.

Salinity values are definitely different between the value from the core of the mineralized zone at Maden River and from the value of the marginal part in the mineralized zone around Maden River; namely, the former values are 40% ~ 50% detected by salt volume in inclusion, and the latter values range from 7% to 20% (freezing point ; -4.2℃ to -15℃) by cooling stage method.

2-3 Conclusion of Measurement Results of Fluid Inclusions

Results of fluid inclusions measured from drill cores and rocks from ground surface is completely summarized in the following table.

Rock name	Amount of sample	Qtz vein		Qtz pheno		Qtz vein+Qtz pheno		Total	%
		Liquid	Gaseous	Liquid	Gaseous	Liquid	Gaseous		
Ande	42	679	71			679	71	750	28
Pg1	90	806	168	578	117	1,384	285	1,669	61
Pg2	15	56	26	152	11	208	37	245	9
Qp1	3			44	11	44	11	55	2
Total	150	1,541	265	774	139	2,315	404	2,719	100
%		66.4		33.6		85.1	14.9	100	

(Qtz :quartz, pheno :phenocryst, unit : piece)

The results of fluid inclusion measurements are summarized as follows:

① Homogenization temperatures of gaseous inclusions are generally 30℃ ～ 50℃ higher than those of liquid inclusions in andesite. On the other hand, in the case of andesite of MJT-1, the former is about 10 ℃ higher in temperature than that of the latter.

② Fluid inclusions in altered porphyritic granite (Pg1) were obtained from quartz veins and quartz phenocrysts. On the surface rock, gaseous inclusions in both quartz are also about 40℃ ～ 50℃ higher in temperature than the liquid inclusion's, but in the core sample, gaseous inclusions are, conversely, 2℃ ～ 10℃ lower in temperature than the liquid inclusion's, showing a similar tendency as the case of andesite. Homogenization temperature of fluid inclusions obtained from quartzs phenocryst of altered porphyritic granite (Pg1) around Hasandere on ground surface is highest. The fact presumes that the part is the center of the intrusive stock body of Pg1. The temperature falls slightly toward the deeper part. The fact that the homogenization temperature increases little by little toward the deeper part presumes that the altered porphyritic granite (Pg1) rock body inclines.

③ The area where boiling phenomena might take place, owing to the presence of many gaseous inclusions, is located at and around the north area of Mat Dere. Fluid inclusions in drill cores around the center are high in salinity since many solid inclusions are observable.

④ Fluid inclusions of Pg2 are higher in homogenization temperature than those of Pg1. Also, gaseous inclusions in the former are smaller in scale than those of the latter.

Table 10 Measurement List of Fluid Inclusions

No 1

Sample No	V/P	Name and Description	Homogeniza.T.		Salinity	
			Pcs	Average	Pcs	Average
AE- 7	V	Qz-vein in andesite	21	409	4	8.7
AE- 8	V	Qz-vein in Pgl	16	308	3	5.8
AE- 8	P	Qz-pheno of Pgl	13	342	2	7.2
AE- 9	P	Qz-pheno of Pgl	13	321	2	10.7
AE-11	P	Qz-pheno of Pgl	20	382	3	9.2
AE-13	P	Qz-pheno of Pgl	10	321	2	6.3
AE-15	V	Py-Qz vein in andesite	20	366	3	8.7
AE-16	V	Py-Qz vein andesite	19	381	3	6.9
AE-18	V	Py-Qz vein in andesite	15	369	*	*
AE-23	V-1	Py-Qz vein andesite	14	362	3	10.8
AE-23	V-2	Mo-Py-Qz vein in andesite	17	349	3	9.2
AE-24	V	Mo-rich Py-Qz vein in and.	20	340	3	7.5
AE-25	V	Mo-rich Py-Qz vein in and.	18	396	3	12.4
AE-31	V	Mo-Py-Qz vein in sili and.	15	381	2	10.8
AE-33	V	Mo-Py-Qz vein in sili and.	14	339	2	7.2
AE-37	V	Py-(Mo)-Qz vein in sili and.	17	391	3	14.3
AE-39	V	Py-Mo-Cp-Cc?-Qz vein in and.	12	342	3	17.7
AE-42	V	(Py)-Qz vein in andesite	10	350	3	12.9
AE-43	V	Qz-vein in sili-ser Pgl	20	401	3	16.5
AE-45	P	Qz-phenocryst of Pgl	15	328	2	9.8
AE-54	P	Unaltered Pg2	20	362	4	12.2
AE-56	P	Unaltered Pg2	20	362	*	*
YY- 5	V	Mo-Qz vein in andesite	22	404	3	11.7
YY- 6	P	Qz-pheno of Pgl	16	377	3	7.5
YY- 9	V	(Py)-Qz vein of Pgl	18	361	4	14.1
YY-12	P	Qz-pheno of unaltered Pgl	14	477	3	17.5
YY-15	V	Py-Qz-vein of Pgl	20	408	3	15.4
YY-15	P	Qz-pheno of Pgl	12	361	2	11.8
YY-18	P	Qz-pheno of Pgl	16	347	3	14.3
YY-33	P	Unaltered Pg2	20	333	*	*
YY-26	V	Py-Qz vein Pgl	15	366	4	14.4
YY-26	P	Qz-pheno of Pgl	13	352	3	17.2
YY-27	V	Py-Qz vein of Pgl	20	405	4	17.1

No 2

Sample No	V/P	Name and Description	Homogeniza.T		Salinity	
			Pcs	Average	Pcs	Average
YY-27	P	Qz-pheno of Pgl	18	403	3	17.2
YY-29	P	Qz-pheno of Pgl	15	396	3	19.5
HY- 1	V	Mo-Qz vein in andesite	20	351	3	11.0
HH- 9	V	Pgl with Mo-Py-Qz vein	20	384	4	8.5
HH-13	P	Qz-pheno of Pgl,Py-diss	16	385	2	9.9
HH-19	P	Qz-pheno of wht-alt Pgl	17	304	3	9.2
HH-21	P	Pgl with Py diss	15	304	3	12.2
HH-24	V	Qz-vein of biotite-alt Pgl	20	391	3	12.2
HH-24	P	Qz-pheno of biotite-alt Pgl	20	510	*	*
HH-27	V	Qz-vein of alt Pgl	20	364	4	8.5
HH-36	P	Qz-pheno of greenish P2	21	344	3	12.2
HH-37	P	Qz-pheno of gry glassy Pg2	17	314	*	*
HH-46	P	Qz-vein wht Pgl	20	415	*	*
HH-46	V	ditto	20	408	3	17.2
HH-47	V	Qz-veinlets of Pgl	18	354	4	17.1
HH-53	V	Qz-veinlets of Pgl	20	357	3	8.1
HH-53	P	Qz-pheno of sili-limo.Pgl	12	400	3	10.5
KY- 1	V	Py-Qz vein in andesite	20	386	3	12.2
KY- 9	V	Py-Qz vein in andesite	20	345	3	10.5
KY-12	V	Mag-Py-Qz vein in andesite	20	361	4	10.3
KY-18	V	Mo-Py-Qz vein in andesite	15	453	*	*
KY-19	V	Mo-Py-Qz vein of Pgl	15	386	3	15.4
KY-19	P	Qz-pheno of Pgl	20	397	3	17.7
KY-20	P	Qz-pheno of Pgl	20	406	4	12.2
KY-21	V	Mo-Qz vein of Pgl	20	390	4	18.0
KY-21	P	Qz-pheno of Pgl	18	383	4	13.1
KY-23	V	Mo-Qz vein of Pgl	20	389	3	12.4
KY-24	V	Mo-Qz vein of biotite Pgl	17	399	*	*
KY-24	P	Qz-pheno of biotite Pgl	17	461	3	20.1
KY-25	P	Pg with Mo-Qz vein	17	413	4	15.8
KY-25	V	Pg with Mo-Qz vein	16	479	3	19.3
KM- 4	V	Qz-veinlets of Pgl	10	467	2	17.9
KM-21	V	Qz-vein(float) from andesite	20	404	4	14.4
KM-25	V	Qz-vein of andesite	17	403	*	*

MJT-1 No 3

Depth(m)	V/P	Name and Description	Homoginiza.T		Salinity	
			Pcs	Average	Pcs	Average
52.8	V	Py-Cp-Qz vein in andesite	20	385	*	*
99.8	V	Py-Mo-Cp vein in andesite	20	375	*	*
138.0	V	Py-Mo-Qz vein in Pgl	20	406	3	17.2
183.3	V	(Mo-Py)-Qz vein in Pgl	20	378	*	*
183.3	P	ditto	15	349	2	12.6
210.5	V	Magnetite-Py-Qz vein in and.	15	392	*	*
222.8	V	Py-Cp-Mo-Qz vein in and.	20	401	4	17.7
290.7	V	Mo-Py-Qz vein in and.	15	420	*	*

MJT-2 No 4

Depth(m)	V/P	Name and Description	Homoginiza.T		Salinity	
			Pcs	Average	Pcs	Average
58.4	V	Mo-Qz vein in andesite	12	365	*	*
68.5	V	Cp-Qz vein in andesite	12	371	*	*
71.8	V	Cp-Mo-Qz vein in andesite	15	393	*	*
129.8	V	Qz vein in andesite	20	383	*	*
145.3	V	Magnetite-Cp-Qz vein in and.	20	398	4	17.1
213.5	V	Mo-Qz vein in and.	20	371	*	*
248.0	V	Mo-Qz vein in and	20	406	4	14.4
255.3	V	Py-Mo-Qz vein in and	15	357	3	12.9
268.5	V	Magnetite-Cp-Qz vein in and.	20	409	4	15.0
272.9	V	Mo-Qz vein in and.	20	401	3	17.2
278.0	P	Porphyritic granite (Pgl)	10	387	*	*
283.4	V	Py-Cp-Qz vein in and.	20	410	*	*

MJT-3 No 5

Depth(m)	V/P	Name and Description	Homoginiza.T		Salinity	
			Pcs	Average	Pcs	Average
10.15	P	Qz-pheno of Pgl	15	404	4	13.8
59.0	V	Cp-(Mo)-Py-Qz vein	18	409	4	16.0
59.0	P	ditto	15	384	*	*
80.3	V	(Mo)-Py-Qz vein in Pgl	18	399	3	12.9
118.7	V	Mo-Qz vein in Pgl	10	440	2	11.8
196.0	V	Cp-Py vein in Pgl	20	428	4	16.8
238.9	P	Pgl with disseminated Cp-Py	20	397	3	17.9
255.6	P	Pl-rich Pgl	17	435	4	15.5
258.0	A	Qz-anhydrite vein in Pgl	15	416	*	*
312.5	P	Qz porphyry	15	422	3	17.9
328.1	P	Qz porphyry with Cp-Py diss.	20	409	4	15.5
378.0	V	Py-Mo-Qz vein in Pgl	10	409	*	*
400.6	P	Qz porphyry with Cp-Py diss.	20	435	4	14.4

Homoginiza.T ; Homoginization Tempercture (℃)

Salinity ; NaCl wt %

* ; Impossible to Measure Salinity of Fluid Inclusion

MJT-4 No 6

Depth(m)	V/P	Name and Description	Homoginiza.T		Salinity	
			Pcs	Average	Pcs	Average
19.0	V	Sericite Pgl with qz(5mm)	20	364	8	13.2
37.7	V	Bio-ser Pgl with qz(5mm)	22	375	9	14.6
60.0	P	Biotite Pgl	20	392	*	*
72.1	P	Chl-bio Pgl	22	367	7	11.7
81.6	V	Chl-bio Pgl with qz(6mm)	22	355	*	*
109.0	P	Bio(chl) Pgl	22	424	*	*
116.8	V	Bio Pgl with qz(8mm)	22	382	6	12.3
180.4	V	Chl-bio Pgl with qz(7mm)	22	379	8	13.8
253.0	V	Chl-bio-ser Pgl with qz(5mm)	22	373	9	14.6
280.7	V	Chl-bio-Pgl with qz(1～2mm)	22	419	*	*

MJT-5 No 7

Depth(m)	V/P	Name and Description	Homoginiza.T		Salinity	
			Pcs	Average	Pcs	Average
5.0	P	Sericite Pgl	22	433	*	*
8.0	P	Sericite Pgl	20	448	6	17.3
36.4	P	Sericite Pgl	22	416	*	*
49.0	P	Sericite Pgl with Cc & Cp	20	423	6	14.5
65.3	V	Sericite Pgl with Cc & Cp	20	421	7	13.3
75.5	V	Mo qz (4mm) in Pgl	20	406	*	*
99.0	P	Sericite Pgl	20	392	*	*
133.4	P	Sericite Pgl	11	386	*	*
141.7	V	Py qz vein (10mm) in andesite	20	380	6	13.5
261.4	V	Mo qz vein (10mm) in andesite	20	409	8	16.8

MJT-6 No 8

Depth(m)	V/P	Name and Description	Homoginiza.T		Salinity	
			Pcs	Average	Pcs	Average
40.0	P	Chl-sericite Pgl	13	382	*	*
73.0	V	Silicified chl-sericite Pgl	20	398	6	10.4
85.3	V	Silicified chl-sericite Pgl	18	385	5	10.9
112.6	P	Intrusive rock (Pg2)	17	406	*	*
113.0	V	Segregated qz in Pg2	20	402	7	13.5
123.0	P	Intrusive rock (Pg2)	20	396	*	*
124.5	V	Segregated qz in Pg2	22	397	8	14.7
128.0	P	Intrusive rock in Pg2	10	414	*	*
136.0	V	Segregated qz in Pg2	20	414	*	*
168.4	P	Intrusive rock (Pg2)	23	401	*	*

MJT-7 No 9

Depth(m)	V/P	Name and Description	Homoginiza.T		Salinity	
			Pcs	Average	Pcs	Average
14.45	P	Sericite Pgl	22	379	5	12.8
16.0	V	Sericite Pgl with qz(5mm)	20	371	*	*
56.0	V	Qz vein(10mm) in Pgl	22	367	7	11.0
74.0	V	Chl-ser Pgl with qz(4mm)	20	419	*	*
105.0	P	Ep-chl-ser Pgl with Mo	21	441	8	16.2
125.0	V	Qz vein(20mm) in Pgl	20	419	7	15.0
166.6	V	Qz vein(20mm) in Pgl	22	374	*	*
190.0	V	Silicified Pgl with qz(3mm)	20	375	7	13.3
244.8	V	Sericite Pgl with qz(2mm)	20	398	7	16.2
300.0	V	Silicified ser-anhydrite Pgl	20	435	9	15.4

MJT-8 No 10

Depth(m)	V/P	Name and Description	Homoginiza.T		Salinity	
			Pcs	Average	Pcs	Average
24.0	V	Mo-qz vein(8mm) in Pgl	22	386	6	13.8
46.6	V	Qz vein(5mm) in Pgl	18	383	*	*
66.1	V	Chl-ser Pgl with Cc and qz	22	396	6	14.9
131.0	V	Mo qz vein(30mm) in Pgl	20	404	*	*
135.0	V	Chl-ser Pgl with qz(3mm)	20	411	*	*
146.35	V	Chl-ser Pgl with qz(6mm)	21	402	7	12.6
184.0	V	Mo qz vein(5mm) in andesite	20	440	3	15.4
225.0	V	Ser-chl Pgl with Mo qz(4mm)	20	422	*	*
274.7	V	Magnetite-Py qz(25mm) in Pgl	20	466	*	*
298.5	V	Mo qz vein(10mm) in Pgl	20	410	7	15.0

Abbreviations

Rock name	Pgl: Altered porphyritic granite	
	Pg2: Unaltered porphyritic granite	
Minerals	Qz :Quartz	Cp :Chalcopyrite
	Ch :Chlorite	Py :Pyrite
	Ser:Sericite	Mo :Molybdenite
	Bio:Biotite	Cc :Chalcocite
	Mag:Magnetite	Cv :Covelline
V/P	V :Quartz vein	P :Quartz phenocryst
Homoginiza.T	Homoginization Tempercture (℃)	
Salinity	NaCl wt %	

* ; Impossible to Measure Salinity of Fluid Inclusion

Table 11 List of Fluid Inclusions in Sampling Items

V/P	Rock Name	Locality of sample	No of Sample	Sample Name
V	Andesite (Zigana F)	Maden dere	15	AE-7,15,16,18,23(V1),23(V2),24,25,31,33,
		Hasan dere	4	KY-1,9,12,18,
		North Mat dere	2	KM-21,25
		MJT-1	7	52.8m,99.8m,138m,183.3m,210.5m,222.8m,290.7m
		MJT-2	11	58.4m,68.5m,71.8m,129.8m,145.3m,213.5m,248m,255.3m,268.5m,272.9m,283.4m
		MJT-5	2	141.7m,261.4m
		MJT-8	1	184.0m
	Porphyritic granite (Pg1)	Maden dere	4	AE-8,43,YY-26,27
		Hasan dere	11	HH-9,24,27,46,47,53,KY-19,21,23,24,25
		Mat dere	3	YY-9,15,KM-4
		MJT-3	6	59m,80.3m,118.7m,196m,258m,378m
		MJT-4	7	19.0m, 37.7m, 81.6m*, 116.8m, 180.4m, 253.0m*, 280.7m
		MJT-5	2	65.3m, 75.5m*
		MJT-6	1	85.3m
		MJT-7	8	16.0m, 56.0m, 74.0m, 125.0m, 166.6m*, 190.0m, 244.8m, 300m
		MJT-8	9	24.0m, 46.6*m, 66.1m, 131.0m*, 135.0*m, 146.35m, 225.0m, 274.7m, 298.5m
	Porphy granite(Pg2)	MJT-6	4	73.0m, 113.0m, 124.5m, 136.0m
			97	
P	Porphyritic granite (Pg1)	Maden dere	6	AE-8,9,11,13,45,YY-6
		Hasan dere	9	HH-13,24,46,53,KY-19,20,21,24,25
		Mat dere	6	YY-12,15,18,26,27,29
		South Hasan	2	HH-19,21
		MJT-1	1	183.3m
		MJT-2	1	278m
		MJT-3	4	10.15m,59m,238.9m,255.6m
		MJT-4	3	60.0m, 72.1m, 109.0m
		MJT-5	6	5.0m*, 8.0m, 36.4m, 49.0m, 99.0m*, 133.4m*
		MJT-6	1	40.0m
		MJT-7	2	14.45m, 105.0m
		MJT-8	-	
	Porphyritic granite (Pg2)	South Hasan	5	HH-36,37,AE-54,56,YY-33
		MJT-6	4	112.6m*, 123.0m, 128.0m, 168.4m*
	Quartz porphyry(Qp1)	MJT-3	3	312.5m,328.1m,400.6m
			53	
			150	

* : Abundance of micro-fluid inclusions

Table 12 List of Homogenization Temperatures and Gaseous and Liquid Phases of Fluid Inclusions

V/P	Rock Name	Locality of sample	Liquid Inclusion		Gaseous Inclusion	
			No of M.I	Homogenization T.	No of M.I	Homogenization T.
V	Andesite(Zigana F)	Maden dere	232	369℃	22	465℃
		Hasan dere	58	363	17	457
		North Mat dere	30	403	7	421
		MJT-1	129	391	1	380
		MJT-2	182	389	12	423
		MJT-5	35	391	5	422
		MJT-8	13	434	7	450
	Porphyritic granite (Pg1)	Maden dere	67	372	4	422
		Hasan dere	189	387	17	441
		Mat dere	42	401	7	447
		MJT-3	36	416	55	406
		MJT-4	130	372	22	416
		MJT-5	38	412	2	435
		MJT-6	13	385	5	384
		MJT-7	147	391	17	424
		MJT-8	144	401	39	437
	Porphy.granite(Pg2)	MJT-6	56	399	26	409
			1,541	387	265	427
P	Porphyritic granite (Pg1)	Maden dere	82	352	5	450
		Hasan dere	127	410	33	482
		Mat dere	75	389	14	430
		South Hasan	32	303	-	-
		MJT-1	15	349	-	-
		MJT-2	10	387	-	-
		MJT-3	43	412	24	410
		MJT-4	52	381	12	415
		MJT-5	92	413	23	444
		MJT-6	8	373	5	396
		MJT-7	42	395	1	400
	Porphyritic granite (Pg2)	South Hasan	87	339	6	478
		MJT-6	65	403	5	400
	Quartz Porphyry(Qp1)	MJT-3	44	426	11	416
			774	386	139	439
			2,315	387	404	431

Table 13 List of Homogenization Temperatures of Fluid Inclusions

V/P	Rock name	Locality of sample	No of Sample	No of Inclusins	Range of Temperature(℃)	Mean value(℃)
V	Andesite(Zigana F)	Maden dere	15	254	250～550	377
		Hasan dere	4	75	280～560	384
		North Mat dere	2	37	340～460	406
		MJT-1	7	130	330～470	391
		MJT-2	11	194	320～500	392
		MJT-5	2	40	340～450	395
		MJT-8	1	20	380～490	440
	Potphyritic granite (Pg1)	Maden dere	4	71	280～450	375
		Hasan dere	11	206	300～580	391
		Mat dere	3	49	330～560	408
		MJT-3	6	91	360～490	410
		MJT-4	7	152	320～460	378
		MJT-5	2	40	350～480	413
		MJT-6	1	18	360～420	385
		MJT-7	8	164	330～480	397
		MJT-8	9	183	380～540	409
	Porphy.granite(Pg2)	MJT-6	4	82	380～470	402
			97	1,806	250～580	
P	Potphyritic granite (Pg1)	Maden dere	6	87	300～570	358
		Hasan dere	9	160	320～660	427
		Mat dere	6	89	290～620	405
		South Hasan	2	32	260～350	303
		MJT-1	1	15	290～420	349
		MJT-2	1	10	340～420	387
		MJT-3	4	67	350～490	411
		MJT-4	3	64	330～450	394
		MJT-5	6	115	340～490	418
		MJT-6	1	13	340～410	382
		MJT-8	–	–	–	–
		MJT-7	2	43	320～460	409
	Porphyritic granite (Pg2)	South Hasan	5	93	380～540	348
		MJT-6	4	70	320～450	403
	Quartz Porphry(Qp1)	MJT-3	3	55	350～490	424
			53	913	260～660	394
			150	2,719	250～660	393

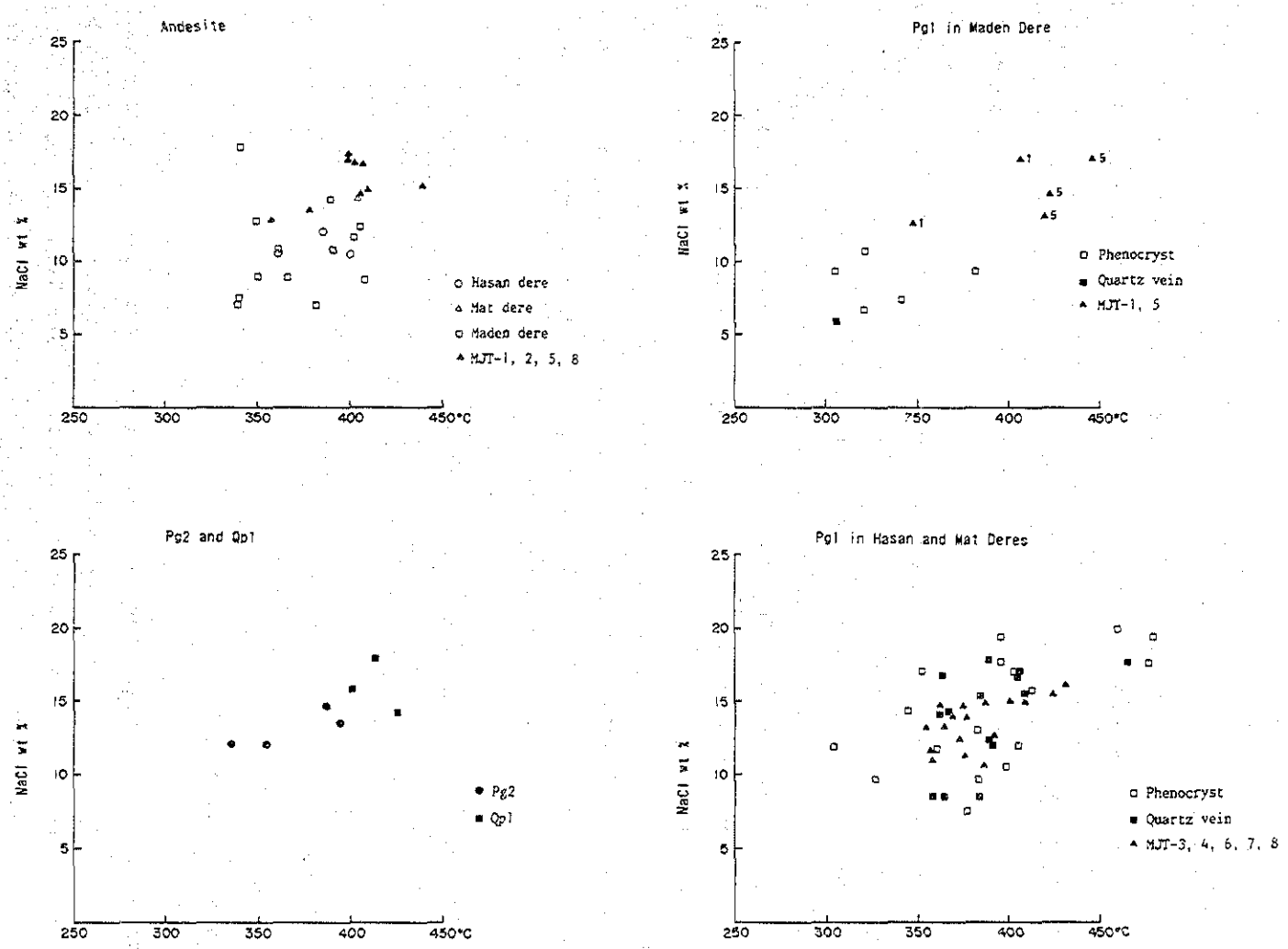

Fig 31 Relationship between Homogenization Temperature and Salinity

⑤ Fluid inclusions have been observed in Pgl at the southern side intruded by PG2.

⑥ A densely saline ore solution was probably supplied to the area of Mat and Hasan Dere.

Chapter 3 Soil Geochemical Survey

3-1 Outline

In 1984, a soil geochemical survey was carried out by MTA at the Hasandere area over an area covering about 3.63 km² from Mat Dere to Hasan Dere. Geochemical anomalies of Cu and Mo reaching 3,820 ppm Cu and 272 ppm Mo in maximum value were discovered. An anomolous area based on a threshold value of 236 ppm Cu was open to the northern area, and the result pointed out the possibility that the area may extend further to the north of the geochemically surveyed area.

Taking this into consideration, MTA continued the soil geochemical survey in the north area. Soil samples were collected from the B or C soil horizon at 50m intervals along each 50 m contour level following the same specifications as the 1984 survey. These samples were analysed for the two elements, Cu and Mo. Total assay results for 1331 samples,(942 samples of the 1984 survey combined with 389 samples from the 1985 survey) were processed through the computer applying the Lepertier method (1969). The data processing method was introduced in detail in the report by the cooperative mineral exploration of the initial phase. Statistic parameters obtained through the data processing are shown in the table described below. Histogams, cumulative frequency and correlation diagrams are shown in Fig. 32.

Element	N	Mean(M)	M+α	M+2α	Min valu	Max value	γ
Cu	1311	66.3	200	602	4	3,820	0.56
Mo	1331	4.4	18	71	<1	272	

3-2 Data Examination

Cu consists of one unit since its cumulative curve is a straight line, shown in Fig. 32. To the contrary, the cumulative distribution curve of Mo has two inflection points, t1 (11ppm) and t2 (27ppm). The form of the histogram and the two inflection points in the cumulative distribution curve indicate that Mo

consists of an anomalous population (larger than t2), a background population (less than t1) and an overlaping population (between t1 and t2).

As shown in the correlation diagram in Fig 32, the coefficiency of correlation between Cu and Mo (γ) is 0.56, a slight correlation. Investigation of the distribution tendency of high values delineated on the equi-contour value map indicates that anomalous zones of Cu and Mo are discordantly distributed. Cu anomalous zones are located on the outer side of Mo anomalous areas, backing up the weak correlation between both elements.

A high Mo anomalous zone was distinct in the area from Mat Dere to Hasan Dere.

An especially anomalous area of higher than ($M+2\sigma$) is found north of MJT-3 drill site located on the north side of Mat Dere. Areas with Cu high anomalies larger than ($M+\sigma$) are indistinctly concentrated, and the distribution is dispersed.

There is no geochemically anomalous area of Mo located downstream of Mat Dere and Hasan Dere. This area coincides with the potassic alteration zone identified by geological and alteration surveys, and is regarded as a barren zone, namely as the core of mineralization of the porphyry copper ore deposit.

A post-mineralization fault on the west side of Maden Dere is inferred by geological survey. Anomalous areas of both elements, Cu and Mo, were not found on the west side of the inferred fault, and the west end of the detected anomalous area extends harmoniously along the inferred fault. This fact consequently reveals the existence of the fault.

Contrary to the fact that the Cu anomalous zone is distributed centered around the stream, the Mo anomalous area is not influenced by topographic conditions. In the case of the forming of the oxide and leached zone in the ore deposit, copper and sulphur are completely leachable by acidic water produced from sulphide minerals such as pyrite through oxidation, and is easily movable, but on the other hand, gold and molybdenum in general are scarcely moved (Bloom, 1966; Shanon Jr.,1971 ; Asami and Britten, 1980). When molybdenite is oxidized, and molybdic acid (MoO_4^{2+}) is produced, the molybdenum is extremely soluble, but if Fe^{3+}ion(low Eh) exists in acid water or if Ca^{2+}ion exists in neutral water, ferrimolybdenite($Fe_2O_3MoO_3 \cdot 8H_2O$) and powellite ($CaMoO_4$) are precipitated and fixed as a mineral phase (Garrels and Christ, 1965). It is presumed that such a difference in the secondary dispersion between copper and molybdenum controls the distribution of the Cu and Mo anomalies. It is expected from the characteristic of Mo for difficult dispersion that the geochemical anomaly of Mo will indicate precisely the mineralization condition (such as grade), and the area with a concentration of high Mo anomalies on the north side of Mat Dere is expected to be the most promising area for emplacement of the ore deposit.

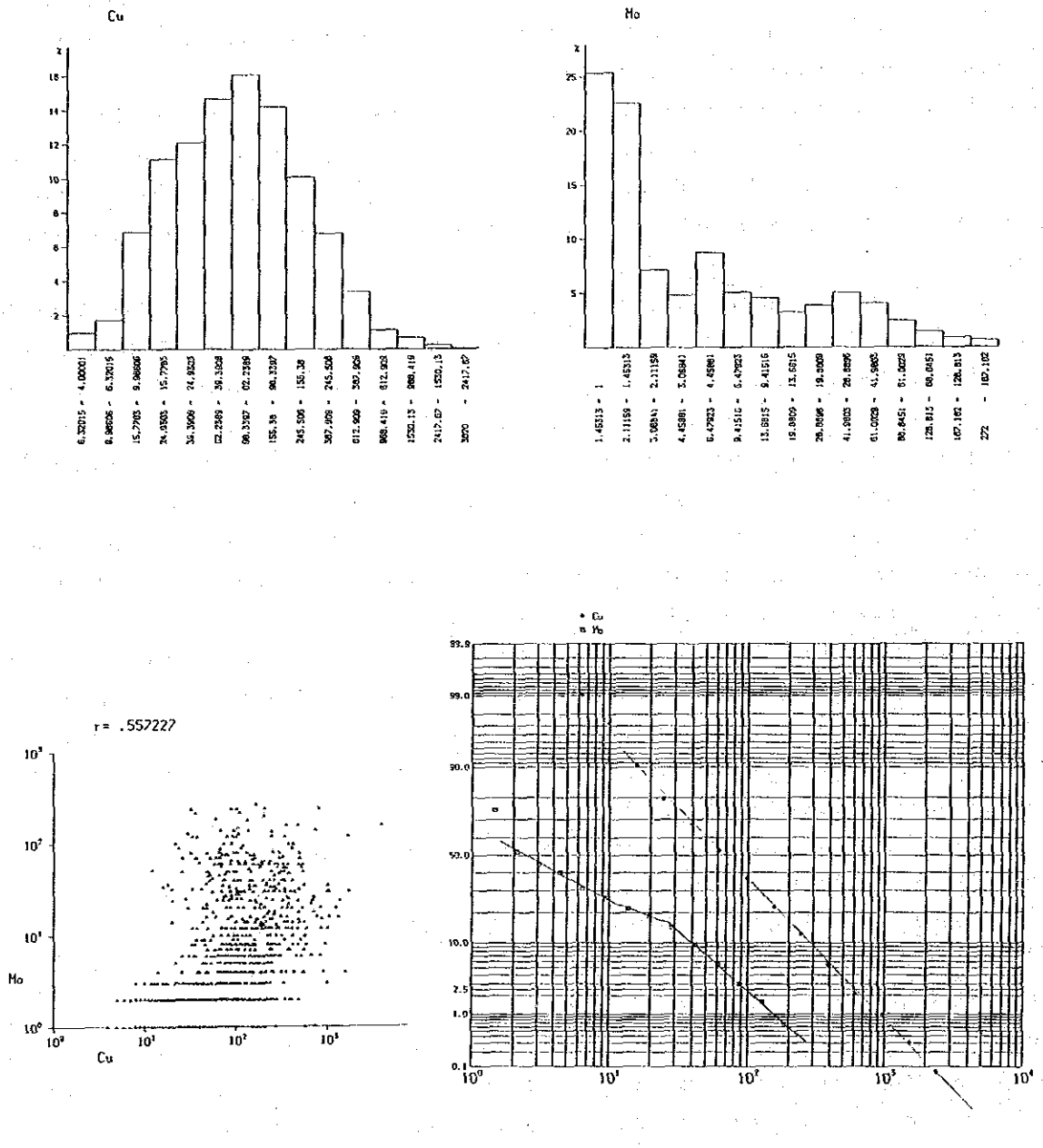

Fig 32 Histogram, Cumulative Frequency Distribution Curve, and Correlation Diagram of Soil Geochemical Survey, Güzelyayla Area

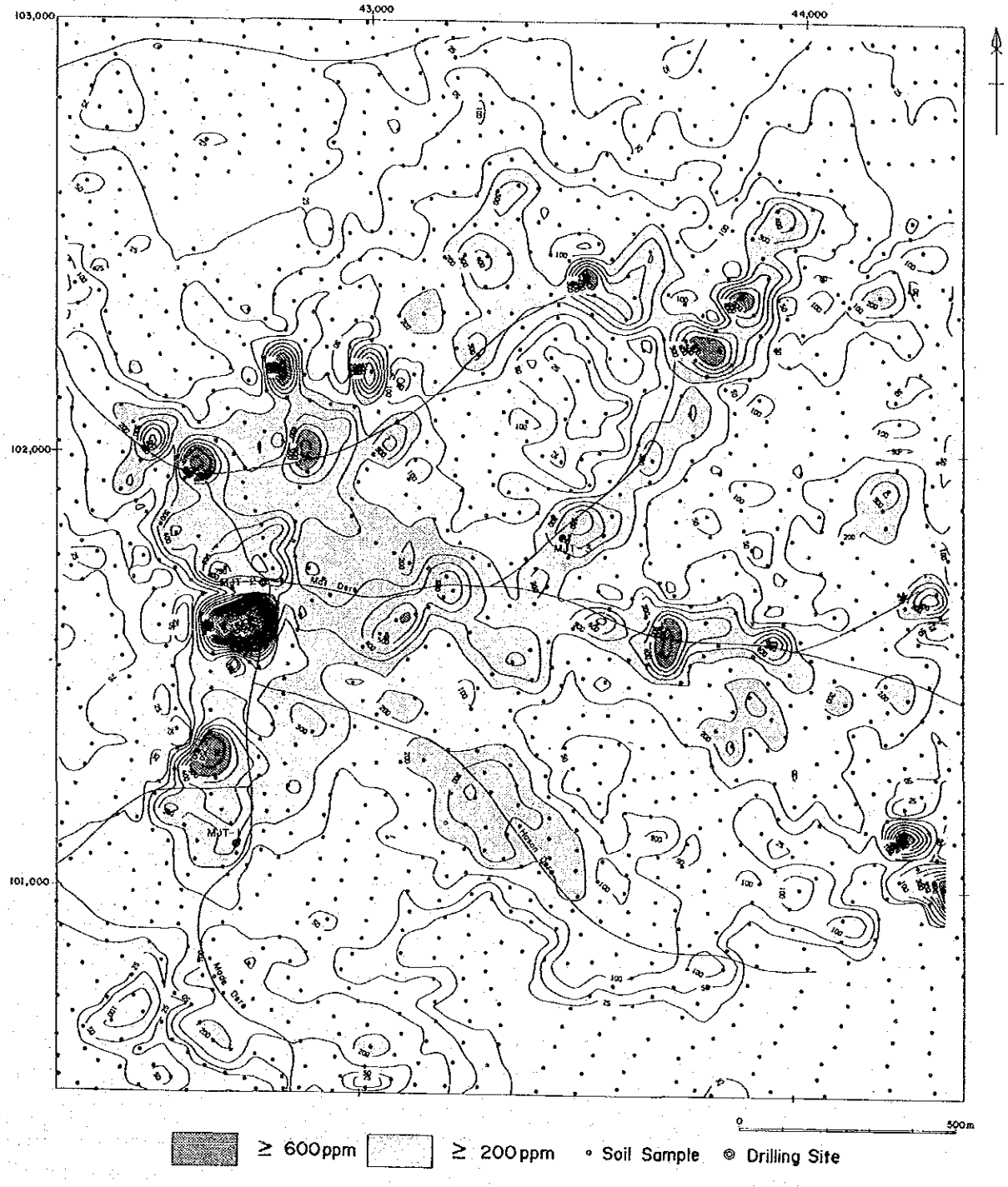

Fig. 33 Soil Geochemical Contour Map of Cu Anomaly in Güzelyayla Area

Mo

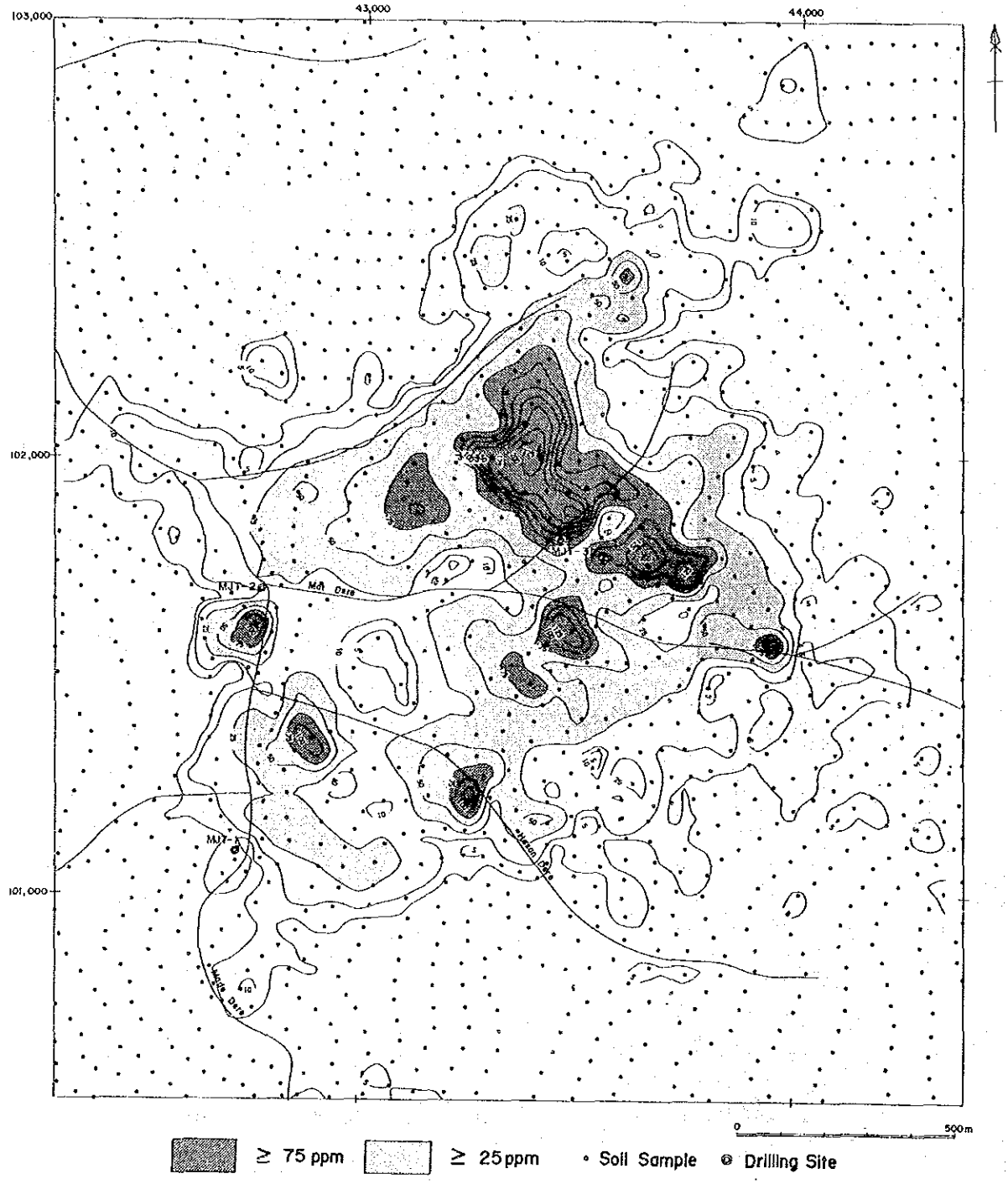

Fig. 34 Soil Geochemical Contour Map of Mo Anomaly in Güzelyayla Area

Chapter 4 Geophysical Survey (SIP and IP Methods)

4-1 Outline of the Survey

Purpose of the Survey : The survey refers to an area where a mineralized zone of porphyry copper type had been found through geological and geochemical surveys of the initial phase. In the second phase, geophysical (SIP) and drilling surveys were successively carried out aimed at exploration of the mineralized zone. The two SIP lines were surveyed for the purpose of determining continuity of the mineralized zone between three drill holes.

In the third phase, the geophysical methods of SIP (three lines) and IP (six lines) were used to unravel the emplacement condition and the continuity of the mineralized area.

Area of the Survey : The target area and arrangement of the survey lines are illustrated in Figs. 2 and 35, respectively.

Length of the Survey Line :

Phase II		3.5km in two lines	
SIP :	Line A 2.0km,	Line B 1.5km	135 points
Phase III		18.0km in nine lines	
SIP :	Line D,G,I	6.0km in three lines	240 points
I P :	Line B,C,E,F,H,J	12.0km in six lines	480 points

4-2 Survey Method

The SIP method is the abbreviated name of the Spectral Induced Polarization method and operates on the same principal as the conventional IP method. The SIP method measures apparent resistivity and phase difference over a frequency range of 0.01 Hz to 100 Hz. Analysis of these responses gives discrimination of minerals or types of mineralization and eliminates electromagnetic coupling.

In this survey, the Harmonic System (Fig.36) of Zonge (USA) was applied.

Survey Specifications : Field work specifications in the second and the third phases were set as follows :

a. Electrode Configuration	dipole-dipole array
b. Electrode Separation	100m
c. Electrode Separation coefficient	n=1～5
d. Measurement Method	Frequency domain

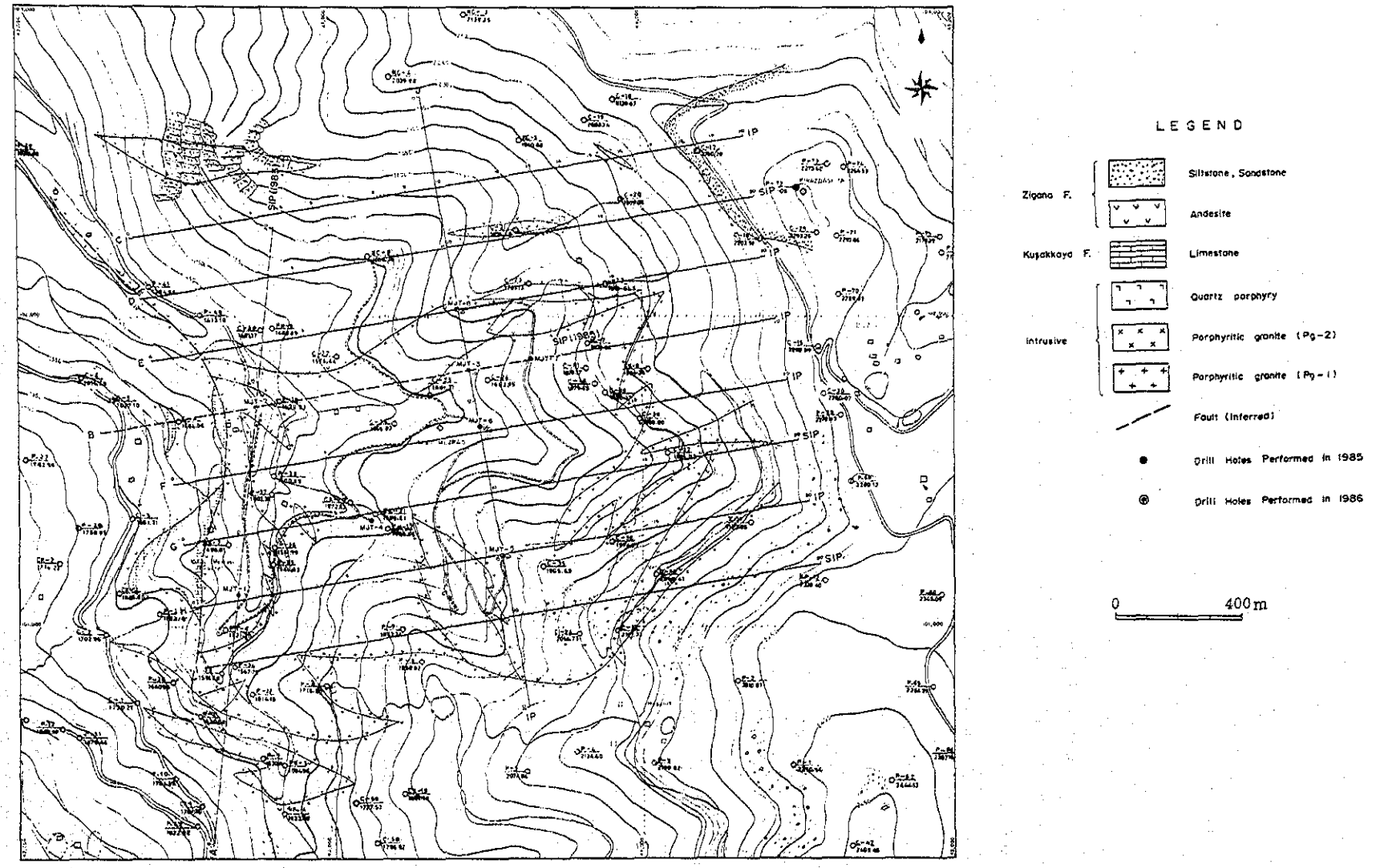

Fig. 35 Location Map of SIP and IP Survey Lines in the Güzelyayla Area

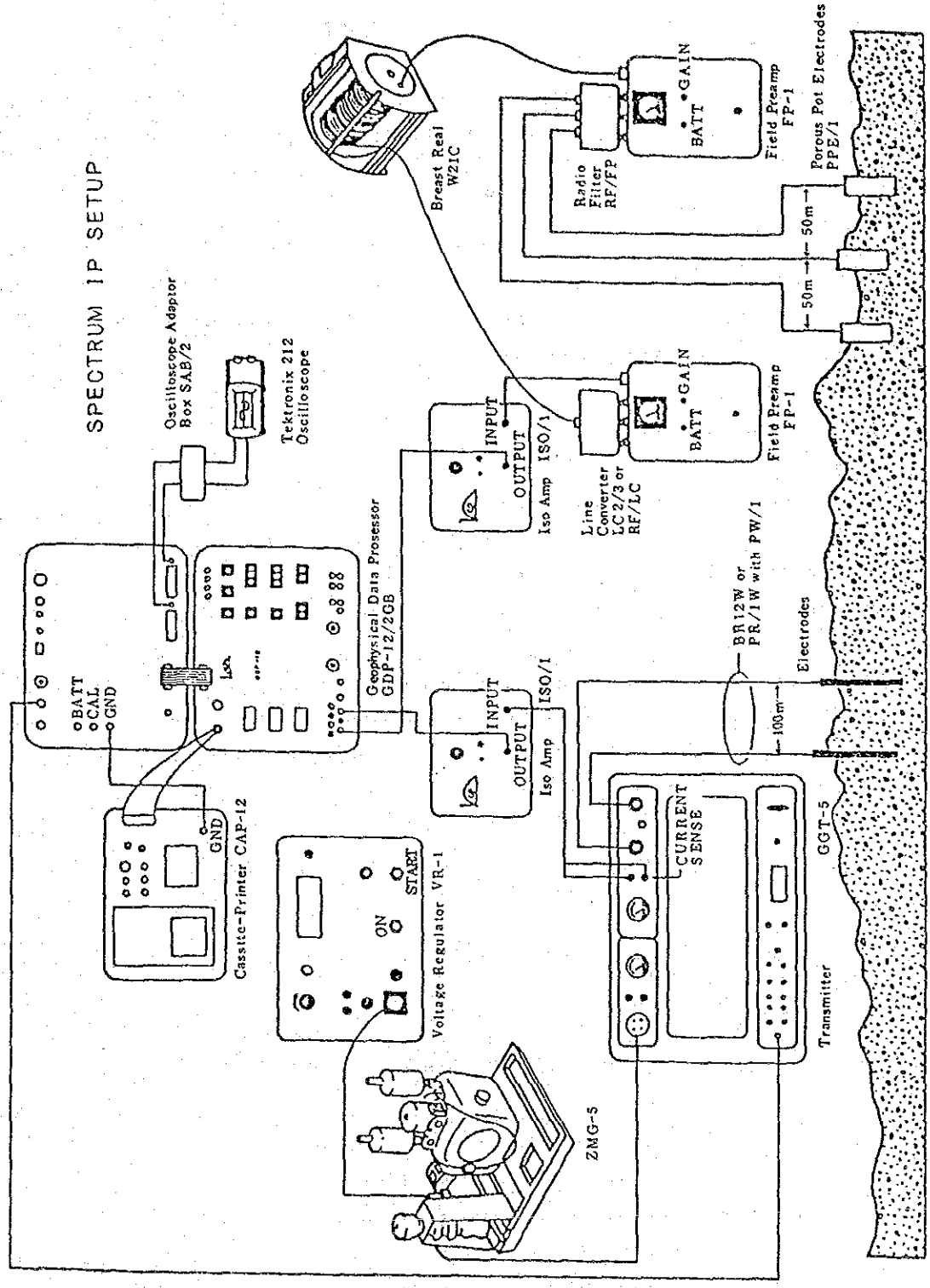

Fig.36 Illustrated Diagram for SIP Equipment

e. Frequencies SIP 0.125 Hz ~ 88 Hz(18 frequencies)
I P 0.125 Hz/ 1.0 Hz

Measuring Equipment : The equipment used in this survey are listed in Table 14. The same equipment loaded with the IP program was used for the IP measurement.

SIP Data Processing : Data obtained in the field consist of real and imaginary parts of complex resistivity response at each frequency, apparent resistivity, phase and magnitude of received basic frequency, and so on. The following figures are determined using these data :

① Cole-Cole Diagram
② Magnitude Spectrum
③ Phase Spectrum
④ Raw Phase at five freqencies
⑤ PFE Pseudo-section
⑥ Apparent Resistivity Pseudo-section

The decoupling process was conducted on data over the whole SIP lines.

IP Data Processing : Panel Diagrams of percent frequency effect (PFE) and apparent resistivity (AR) were provided from pseudo-sections of each line. Three plan maps were prepared on each electrode separation coefficient of n=1, 3, 5.

A) PFE

A value of PFE is calculated by magnitudes (M) at 0.125 Hz and 1 Hz as follows :

$$PFE = \frac{M(0.125\ Hz) - M(1.0\ Hz)}{M(0.125\ Hz)} \times 100 \quad (\%)$$

B) AR

A value of AR is calculated by the following equation :

$$AR = \pi a \cdot n(n+1)(n+2) \cdot V/I \quad (ohm\text{-}m)$$

where, a : electrode separation in meters
n : electrode separation coefficient
V : voltage received in volts
I : transmitted current in amperes

In the present survey, the apparent resistivity at 0.125 Hz was calculated and topographic correction was made with conductive paper.

Table 14 List of Measuring Equipment for SIP and IP Survey

Item	Specification		Quantity
Zonge GGT-5 Transmitter	Output Voltage Output Ampere Wave Form Frequency Weight	: 250, 500, 750, 1,000 V : 1.2 - 20 A : Square wave : 1/8 - 2,048 Hz : 61 Kg	1
Zonge XMT-12 Transmitter controller	Frequency Weight Power Supply	: 1/8 - 2,048 Hz : 58 Kg : 12 V Battery	2
Zonge ZMR-5 Engine generator Honda G-400 Engine	Output Power Output Voltage Frequency 	: 5 Kw : 115 V : 400 Hz : 10 hp 4 cycles	1
Zonge GDP-12/2GB Receiver	Input Frequency Senstivity Weight Power Supply	: 2-Channel : 1/8 - 2,048 Hz : 0.2 μV : 15 Kg : 12 V Battery	2
Zonge CAP-12 Mini Cassette Recorder	Weight Power Supply	: 6.2 Kg : 12 V Battery	2
Tektronic 212 Oscilloscope			1
Zonge ISO/1 Isolation Amp.	Weight	: 1 Kg	3
Zonge FP-1 Feild Preamp.	Gain	: 1, 10	3
Electrode	Current Electrode Potencial Electrode	: Stainless steel : Cu-$CuSO_4$ non-polarizable Porous Pots	200 rods 10 pcs.
Cable	Current Communication	: : 640 m length	10 Km 3 rolls

4-3 Results of the geophysical survey

Rock Sample Measurement : The main rocks distributed in the surveyed area and drill cores were tested in the laboratory. The number of samples is as follows:

Phase II : Rocks 16 pieces
Cores 19 pieces from MJT-1 ~ MJT-3
Phase III : Cores 25 pieces from MJT-4 ~ MJT-8

The results shown in Table 15 for each rock type indicate the following : The results from these samples can be categorized by their phase spectra which fall into seven types as A, B, C, D, E, X and Y .

The result indicates the following :

① Phase and PFE values of andesite and basaltic andesite are the highest. The next is porphyritic granite. In the same rock, these values vary extensively in range depending on condition of alteration and pyrite dissemination.

② Phase and PFE are proportionately correlated.

③ Resistivity values are in a wide range from 126 ohm-m to 12,650 ohm-m. Most values are generally high, but 10 samples (17 % of the total 60 samples) are below 500 ohm-m.

④ In the case of the phase spectrum, samples of high phase and PFE belong to the X and Y types. Resistivity is not correlated with the phase spectrum.

⑤ On the other hand, weakly mineralized or fresh rock samples are higher than 2,000 ohm-m in resistivity, and mostly belong to A and D types of the phase spectrum.

⑥ In comparison, types in the Cole-Cole diagram are divided into two groups, one belonging to type C in the Cole-Cole diagram containing A,B,C and D types of phase spectra and the other belonging to type A in the Cole-Cole diagram containing E, X and Y types of phase spectra.

Rock properties of 44 drill cores are given in Table 16. The relation between phase and metal content of Cu and Mo is shown in Table 17. Rock properties of each phase type are given in Table 18.

The following items are pointed out.

① A specific type of phase spectrum does not correspond with specific metal contents of copper or molybdenum, but copper rich samples have a tendency to show a spectrum of A-, B- or D-type. Samples rich in

Table 15 Results of Rock and Core Sample Measurement (GÜzelyayla Area)

Rock	Sample No.	Phase (-mrad)	PFE (%)	Resistivity (ohm-m)	Phase spectrum type						
					A	B	C	D	E	X	Y
Andesite											
Andesite	13	-4.3～56.16	-0.19～144.57	126～10,068	4			4		3	2
		(109.6)	(25.68)	(1,753)							
		(10.1)※	(1.73)※	(1,976)※							
Basaltic Andesite	6	3.5～376.2	0.45～88.31	547～7,164	2	1		1		2	
		(108.5)	(22.20)	(3,970)							
		(14.3)※	(2.19)※	(5,408)※							
Pyroclastic Andesite	3	3.9～5.1	0.58～0.73	1,819～4,996	3						
		(4.4)	(0.63)	(3,828)							
Porphyritic granite											
Pg-1	28	7.8～208.8	0.40～38.71	195～7300	5	4		11	3	2	3
		(38.5)	(5.97)	(2,281)							
Pg-2	5	17.5～40.1	2.40～ 6.00	405～6,551	1	3			1		
Qurtz Porphyry											
	1	6.5	0.84	5,207			1				
Qurtz vein											
	1	13.8	2.20	3,120	1						
Calcareous mudstone											
	1	10.1	1.16	4,322			1				
Siltstone											
	2	1.9～ 2.4	0.32～0.34	3,273～12,649	2						
Total	60				18	8	2	16	4	7	5

( ) Average value

※ Excepted anomalous value

Table 16 Results of Core Sample Measurement and Cu, Mo %

Sample No.	Depth (m)	Rock	Phase (-mrad)	PFE (%)	Resist. (ohm-m)	Spectrum type	Cu (%)	Mo (%)	Remarks
Drilling No. MJT - 1									
21	52.10	Alternated andesite	-2.2	0.50	162	D	0.06	0.001	Sericite-chlorite,diss.pyrite
22	99.80	Alternated andesite	-4.3	-0.19	126	D	0.09	0.009	Diss.pyrite
23	139.90	Porphyrtic granite(pg1)	21.8	4.56	219	D	0.08	0.004	Pyrite-quartz vein
24	150.80	Alternated andesite	561.6	134.17	449	Y	0.10	0.001	Epidote, pyrite along fissures
25	184.50	Porphyrtic granite(pg1)	208.2	38.71	1,795	X	0.09	0.019	Diss.pyrite
26	200.10	Basaltic andesite	3.5	0.45	4,757	A	0.06	0.001	Propyliza.
27	250.90	Andesite	8.8	1.43	1,299	A	0.03	0.00	Filmy pyrite
28	274.30	Basaltic andesite	117.8	18.20	547	X	0.04		Propyliza.,diss.pyrite
29	297.90	Basaltic andesite	376.2	88.31	1,361	X	0.01		Propyliza.,diss.pyrite
Drilling No. MJT - 2									
31	44.70	Porphyrtic granite(pg1)	7.8	1.60	294	D	0.15	0.003	Diss.pyrite,sericite-chlorite
32	51.70	Alternated andesite	6.7	1.49	824	B	0.40	0.010	Propyliza.,diss.pyrite
33	154.30	Alternated andesite	541.2	144.57	550	X	0.12	0.003	Diss.pyrite along fissures
34	200.00	Alternated andesite	221.2	37.22	2,035	Y	0.12	0.004	Diss.pyrite along fissures
35	250.10	Alternated andesite	21.2	3.30	10,068	A	0.19	0.008	Diss.pyrite along fissures
36	299.30	Basaltic andesite	32.1	4.91	4,303	B	0.13	0.004	Diss.pyrite along fissures
Drilling No. MJT - 3									
41	151.05	Porphyrtic granite(pg1)	36.7	5.53	849	A	0.21	0.006	Sil.,sericite,molybdenite-qz
42	199.20	Porphyrtic granite(pg1)	32.4	4.69	3,754	B	0.15	0.011	Sil.,sericite,diss.pyrite
43	250.00	Porphyrtic granite(pg1)	19.4	3.08	6,253	B	0.13	0.007	Sil.,molybdenite,diss.pyrite
44	301.20	Porphyrtic granite(pg1)	38.6	0.83	1,694	X	0.07	0.004	Sil.,sericite,diss.pyrite
Drilling No. MJT - 4									
1	16.5	Porphyrtic granite(pg1)	31.1	4.3	797	B	0.21	0.001	Diss.pyrite, sericite-biotite
2	52.0	Porphyrtic granite(pg1)	83.1	13.3	990	D	0.06	0.002	Chalcopyrite, diss.pyrite, biotite-chlorite
3	100.0	Porphyrtic granite(pg1)	8.5	0.4	360	E	0.02	0.000	Sericite-biotite-chlorite
4	500.0	Porphyrtic granite(pg1)	41.8	6.3	1,390	D	0.05	0.000	Diss.pyrite, biotite-sericite
5	200.0	Porphyrtic granite(pg1)	17.7	2.3	258	D	0.05	0.002	Sericite-chlorite-biotite
6	250.0	Porphyrtic granite(pg1)	28.7	3.7	852	Y	0.04	0.005	Biotite-sericite
7	300.0	Porphyrtic granite(pg1)	19.5	2.4	1,100	Y,(E)	0.04	0.010	Sericite-biotite-chlorite
Drilling No. MJT - 5									
8	49.0	Porphyrtic granite(pg1)	63.0	9.3	3,560	A	0.05	0.000	Chalcocite, Chalcopyrite, sericite
9	99.0	Porphyrtic granite(pg1)	41.2	6.6	2,160	D	0.03	0.000	Sericite
10	195.0	Basaltic andesite	114.0	20.2	5,690	D,(B)	0.06	0.000	
Drilling No. MJT - 6									
11	13.3	Porphyrtic granite(pg1)	27.9	3.8	1,440	B	0.35	0.024	Sericite
12	49.8	Porphyrtic granite(pg2)	24.7	3.6	1,630	B	0.04	0.000	Diss.pyrite
13	100.05	Porphyrtic granite(pg1)	18.7	2.5	892	D,(E)	0.31	0.010	Sericite-chlorite
14	150.0	Porphyrtic granite(pg2)	17.5	2.6	3,720	B	0.01	0.000	
15	198.8	Porphyrtic granite(pg2)	40.1	6.0	1,580	B	0.06	0.000	
16	250.0	Porphyrtic granite(pg1)	27.6	5.2	889	D	0.19	0.014	
17	301.0	Porphyrtic granite(pg2)	20.5	2.4	405	E	0.09	0.002	Silicified
Drilling No. MJT - 7									
18	16.0	Porphyrtic granite(pg1)	16.4	2.7	7,300	D	0.16	0.013	Sericite, qurtz vein
19	55.0	Porphyrtic granite(pg1)	54.5	10.2	2,530	D	0.05	0.020	Sericite
20	255.0	Porphyrtic granite(pg1)	47.9	8.3	1,600	D	0.15	0.018	Sericite, qurtz vein
21	300.0	Porphyrtic granite(pg1)	62.7	8.7	4,200	Y	0.10	0.006	Sericite-anhydrite
Drilling No. MJT - 8									
22	36.5	Porphyrtic granite(pg1)	24.0	3.7	6,700	A	0.03	0.001	Sericite
23	46.6	Qurtz vein	13.8	2.2	3,120	A	0.04	0.000	
24	146.35	Porphyrtic granite(pg1)	20.3	2.7	911	E	0.08	0.015	Sericite, qurtz vein
25	190.1	Porphyrtic granite(pg1)	31.2	3.9	195	E	0.14	0.008	Sericite, qurtz vein

1985 : MJT-1,-2,-3
1986 : MJT-4,-5,-6,-7,-8

Table 17 Relationship between Cu, Mo % and Phase Spectrum

	SPECTRUM TYPE						
Cu (%)	A	B	C	D	E	X	Y
≦ 0.02		1				1	
≦ 0.04	3	1		1	1	1	2
≦ 0.06	2	1		6			
≦ 0.08				1	1	1	
≦ 0.10				1	1	1	2
≦ 0.12						1	1
≦ 0.14		2			1		
≦ 0.16		1		3			
≦ 0.18							
≦ 0.20	1			1			
≦ 0.22	1	1					
≦ 0.24							
≦ 0.26							
≦ 0.28							
≦ 0.30							
≦ 0.40		1		2			
Total No.	7	8		15	4	5	5

	SPECTRUM TYPE						
Mo (%)	A	B	C	D	E	X	Y
≦ 0.002	5	4		6	2	2	1
≦ 0.004		1		2		2	1
≦ 0.006	1				1		2
≦ 0.008	1	1					
≦ 0.010				3		1	
≦ 0.012		1					
≦ 0.014				2			
≦ 0.016					1		
≦ 0.018				1			
≦ 0.020				1		1	
≦ 0.022							
≦ 0.024		1					
≦ 0.026							
≦ 0.028							
≦ 0.030							
≦ 0.040							
Total No.	7	8		15	4	5	5

Table 18 SIP Response and Cu, Mo % in the Classification of Phase Spectrum

Type	Sample No.		Phase -mrad	PFE %	Resistivity ohm-m	Cu %	Mo %
A	7	Min.	3.5	0.45	849	0.03	0.000
		Max.	63.0	9.30	10,068	0.21	0.008
		Ave.	24.3	3.70	4,336	0.09	0.002
B	8	Min.	17.5	2.60	797	0.01	0.000
		Max.	40.1	6.00	6,253	0.35	0.024
		Ave.	28.2	4.12	2,934	0.14	0.006
D	15	Min.	-4.3	-0.19	126	0.03	0.000
		Max.	114.0	20.20	7,300	0.40	0.020
		Ave.	32.8	5.70	1,688	0.13	0.007
E	4	Min.	8.5	0.40	195	0.02	0.000
		Max.	31.5	3.90	911	0.14	0.015
		Ave.	20.1	2.40	468	0.08	0.006
X	6	Min.	38.6	0.83	449	0.01	0.001
		Max.	541.2	144.57	1,795	0.12	0.019
		Ave.	307.3	70.80	1,066	0.07	0.005
Y	4	Min.	19.5	2.40	852	0.04	0.004
		Max.	221.2	37.22	4,200	0.12	0.010
		Ave.	83.0	13.00	2,047	0.08	0.006

molybdenum often show a spectrum of B-, D- or E-type. But, types of A, B, D and E are also common in samples of poor Cu and Mo content, making it difficult to presume a metal content by one of these types.

② X- or Y-type, which are popular in massive ores, has been observed in samples of low Cu or Mo content, but it is noticed that samples of these types have not been detected in samples with high Cu or Mo content. Samples of X- or Y-types in this area are megascopically rich in pyrite. Spectra of these types can be related with pyrite mineralization.

③ According to Table 18, phase spectra of high copper content are of B- and D-types and these are followed by A- , E- or Y- , and X-types in descending order. The copper content of B- and D-types are some 1.7 times larger than that of others. The phase stands at about 30 mrad with a value of 4 to 6 % PFE. Molybdenum contents are highest with D-type, moderate with B-, E- and Y-type spectra and the lowest with A-type.

④ Samples of X-type spectra are rather poor in Cu and Mo contents.

Consequently, samples with high copper content often show a B- or D-type spectrum with moderate values of phase, PFE and AR. Samples associated with X- or Y-type are related with pyrite mineralization with a low value of Cu or Mo.

Due to low values of metal content, copper and molybdenum did not give a specific spectrum. It is possible that the specific spectrum is obtained if samples have more metal content.

Results of field measurements : The survey is comprised of the measurements of SIP over five lines totalling 9.5km and IP over six lines totalling 12km with a line interval of 200m to delineate the extension of the mineralized zone.

Results of field data were interpreted with the plans and sections of apparent resistivity and PFE respectively, and with SIP response and model simulation.

Results of the interpretation is shown in Fig. 39 and indicate the following:

1) A R (Fig.37)

① Prevailing AR are of the order of 200～500 ohm-m.

② Zones of AR less than 100 ohm-m have been detected mainly in the vicinities of Maden Dere in the west and Hasan Dere in the south. These zones are situated in areas of andesites and the porphyritic granite (Pgl), and are probably related with alteration zones and ground-water.

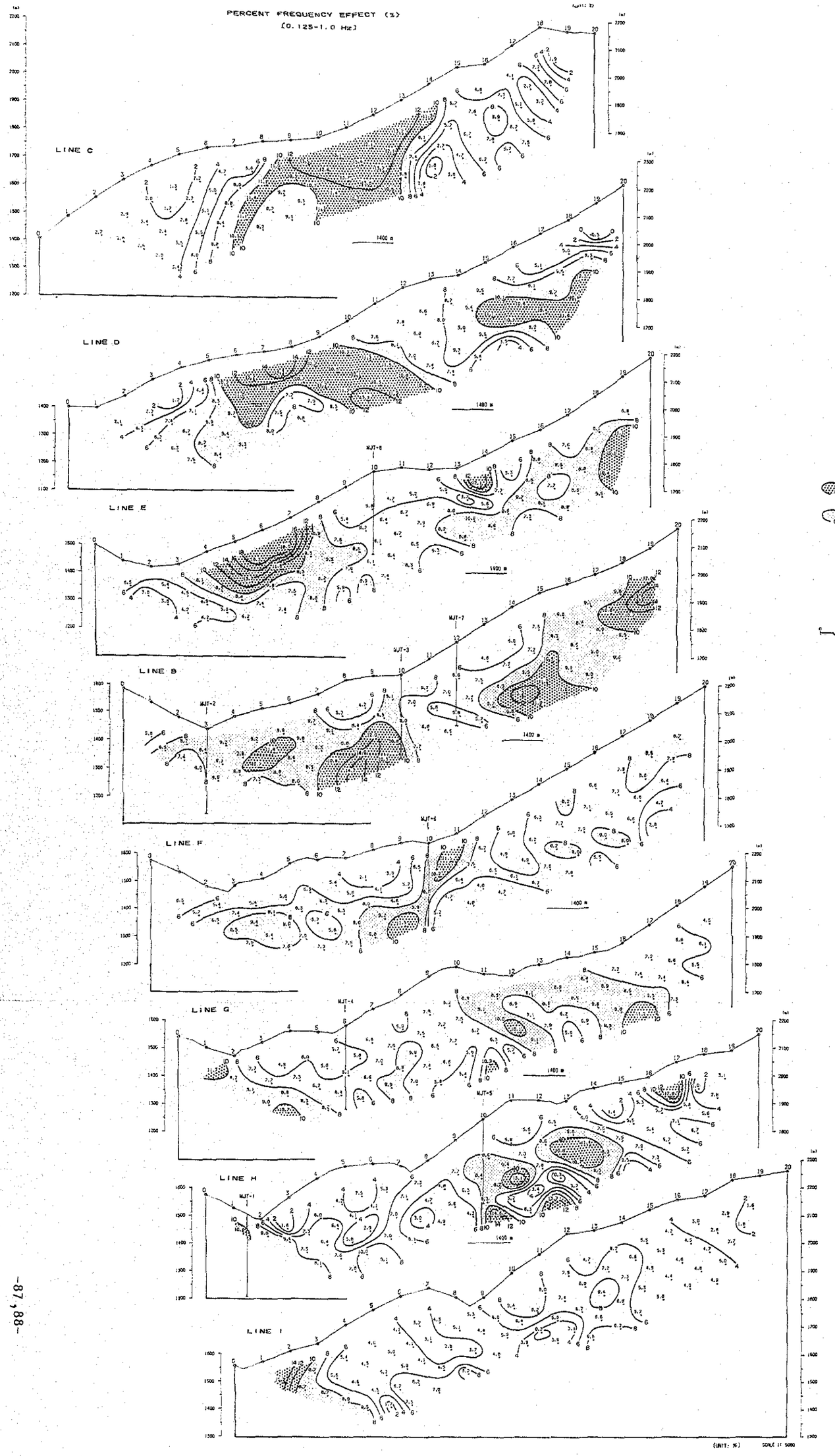

Fig. 38 Panel Diagram of PFE [0.125-1.0 Hz] (Line B~I)

③ Zones of high AR are located between No.6 and No.9 and between No.13 and No.17 of Line C in the north and east of Lines H and I in the south-eastern part of the area where andesites and porphyritic granites underlie.

2) PFE (Fig.38)

① The PFE stands as an indicator of the extension of the mineralized zone and more than 90% of the PFEs exceed a level of 4%.

② The laboratory investigation of surface rock samples and cores conducted in the previous year showed that the PFE of fresh rocks or weakly mineralized samples did not exceed 1.5%. A zone of 4% PFE can be deemed anomalous, suggesting that the whole area belongs to a mineralized zone.

③ A zone of more than 8% PFE gives a horseshoe shape distribution in the northern half of the area, and another zone of high PFE has been detected in the central part of the area extending southward. A pyrite shell is found on the outer side of the phyllic alteration zone and a bonanza of copper and molybdenum is located inside the pyrite shell.

④ The horseshoe shape zone of more than 8% PFE at n=1 can be correlated with the pyrite shell and roughly coincides with a phyllic zone, and is assumed to extend to the poximity of Line D in the north-eastern area as indicated by this investigation.

3) SIP response : The following matters are pointed out from the measuring of five SIP lines.

① Generally, Phase spectra showed A and B-type in the whole SIP line, and negative phase spectrums are detected between stations No.6 and No.11. The X- and Y-type are detected in the same place in the high PFE zone, and originate from strong pyrite dissemmination in the phyllic zone.

② The Magnitude spectrum is generally of a decreasing nature with a small inclination. A larger inclination has been detected in the same place where X- and Y-type in phase apppeared

③ The Cole-Cole diagram indicated an almost B-type with a flat spectra. A-type originated at the same place as X- and Y-type where strong mineralization was detected .

④ The characteristic SIP responses originated with pyrite. Due to low value of metal content, the copper and molybdenum did not give a specific spectrum.